AD-A107 910 OFFICE OF NAVAL RESEARCH WESTERN REGIONAL OFFICE PAS--ETC F/G 8/10
ARABIAN SEA PROJECT OF 1980: COMPOSITES OF INFRARED IMAGES.(U)
AUG 81 B J CAGLE, R WHRITNER
UNCLASSIFIED ONRWEST-81-5 NL

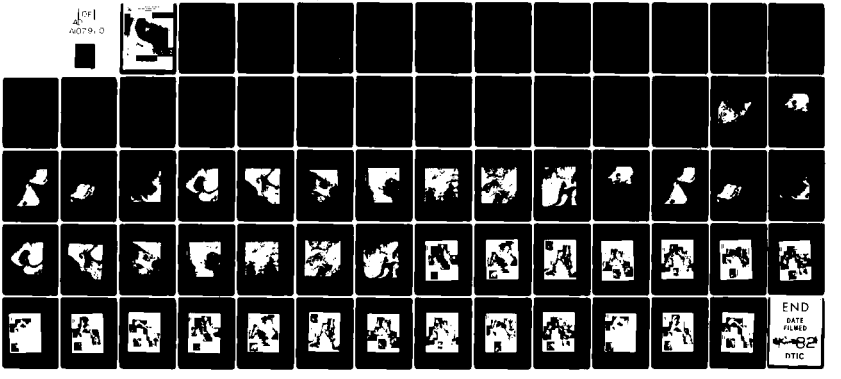

Cover: Infrared (3.55 to 3.93 μm) image of the Gulf of Oman, Arabian Sea, obtained by NOAA-6 Satellite on 30 May 1980 and enhanced in the Scripps Institution of Oceanography Remote Sensing Facility.

UNCLASSIFIED

SECURITY CLASSIFICATION OF THIS PAGE (When Data Entered)

12-61

REPORT DOCUMENTATION PAGE		READ INSTRUCTIONS BEFORE COMPLETING FORM
1. REPORT NUMBER ONRWEST Report-81-5	2. GOVT ACCESSION NO. AD-A107 116	3. RECIPIENT'S CATALOG NUMBER
4. TITLE (and Subtitle) ARABIAN SEA PROJECT OF 1980: COMPOSITES OF INFRARED IMAGES		5. TYPE OF REPORT & PERIOD COVERED Technical Report 6. PERFORMING ORG. REPORT NUMBER
7. AUTHOR(s) Ben J. Cagle and Robert Whritner		8. CONTRACT OR GRANT NUMBER(s)
9. PERFORMING ORGANIZATION NAME AND ADDRESS		10. PROGRAM ELEMENT, PROJECT, TASK AREA & WORK UNIT NUMBERS
11. CONTROLLING OFFICE NAME AND ADDRESS Office of Naval Research Western Regional Office 1030 East Green St., Pasadena, California 91106		12. REPORT DATE August 1981 13. NUMBER OF PAGES
14. MONITORING AGENCY NAME & ADDRESS(if different from Controlling Office) Chief of Naval Research Department of the Navy Arlington, Virginia 22217		15. SECURITY CLASS. (of this report) UNCLASSIFIED 15a. DECLASSIFICATION/DOWNGRADING SCHEDULE

16. DISTRIBUTION STATEMENT (of this Report)

Approved for public release; distribution unlimited.

17. DISTRIBUTION STATEMENT (of the abstract entered in Block 20, if different from Report)

18. SUPPLEMENTARY NOTES

19. KEY WORDS (Continue on reverse side if necessary and identify by block number)

Infrared Imagery
Arabian Sea
Remote Sensing

20. ABSTRACT (Continue on reverse side if necessary and identify by block number)

A technique was developed for determining the mesoscale features of the Arabian Sea, and reported on in ONRWEST Report 81-3. A method for assembling composites of images in mosaic form is presented. Enhanced images are presented with surface interpretations for the spring and fall transition periods related to the Northeast and Southwest Monsoons, respectively.

DD FORM 1 JAN 73 1473 EDITION OF 1 NOV 65 IS OBSOLETE
S/N 0102-LF-014-6601

UNCLASSIFIED

SECURITY CLASSIFICATION OF THIS PAGE (When Data Entered)

ONRWEST 81-5

ARABIAN SEA PROJECT OF 1980--COMPOSITES OF INFRARED IMAGES

This report was prepared by
Mr. Ben J. Cagle, ONRWEST
and
Mr. Robert Whritner, Scripps Institution of Oceanography.

Office of Naval Research
Western Regional Office
1030 East Green Street
Pasadena, CA 91106

August 1981

APPROVED:

Lewis Larmore
LEWIS LARMORE
Scientific Director

SUMMARY

A technique was developed to use satellite infrared imagery to describe the mesoscale features of the Arabian Sea (ONRWEST Report 81-3, "Arabian Sea Project of 1980--The Development of Infrared Imagery Technique.") This report discusses the product and interpretation of images.

The data are presented in the form of composites of enhanced infrared images to provide a mosaic of the surface of the Arabian Sea for selected dates in 1980. The composites of images are provided both with and without surface interpretations. The data were selected to show, primarily, the waxing and the waning of the summer Southwest Monsoon. Data obtained during the spring and fall of the year are sufficient to speculate on both the strong effects of the summer Southwest Monsoon and the benign characteristics associated with the winter Northeast Monsoon. In addition, the individual images of one composite of images are provided to illustrate the detail of the enhancement and interpretation of data.

The mesoscale features of the northwestern portion of the Arabian Sea appear to be controlled both by the forcing functions created by the monsoons and by topographic features associated with the coastlines and points of land. There is some evidence of upwelling throughout the year, and warm and cold eddies appear to strengthen and weaken without substantial advection.

SUMMARY

TABLE OF CONTENTS

Acknowledgments:

This development of satellite infrared imagery interpretations was fostered by Dr. Robert Stevenson, Mr. Ben Cagle, and Mr. Robert Lawson of ONRWEST, with the assistance of many people. The lead scientist in the interpretations was Mr. Robert Whritner of the Scripps Institution of Oceanography. This project was funded by ONR Headquarters, the Navy Science Assistance Program, and ONRWEST. The map in Figure 1 was prepared by Ms Jeanne Carleton of the Scripps Institution of Oceanography. This report was typed and proofread by Mrs. JoAnn Harper of ONRWEST.

LIST OF FIGURES

Titles and Identifying Descriptions

Figure 1. Map of Arabian Sea.

The Arabian Sea is bounded on the west by the Arabian Peninsula, on the north by the coasts of Iran and Pakistan, and on the east by the coast of India. Bathymetry is provided down to 3000 meters to illustrate the rapid falloff of the shelf in some areas. The Oman Basin is partially closed by the Murray Ridge with an opening to the Arabian Sea near the Arabian Coast.

Figure 2. Points of Reference.

These points of reference are used to identify possible topographic effects and to give location to features in the infrared images.

Figure 3. Satellite Infrared Image of the Arabian Sea.

This is a low resolution, infrared image obtained from Channel Three of the NOAA-6 satellite on 26 October 1980 (Julian day 300). An ocean thermal feature appears in the center of the view. Both white and black in the image represent saturated data. Clouds appear in the lower and right hand portions of the image. $5^{\circ}x5^{\circ}$ grid spacing.

Figure 4. Persian Gulf.

The lower portion of the Persian Gulf is shown from the vicinity of Qatar to Abu Dhabi. A faint ocean thermal feature appears in the center. The white is saturated data, especially west of Qatar. $2^{\circ}x2^{\circ}$ grid spacing.

Figure 5. Strait of Hormuz.

The vicinity on both sides of the Strait of Hormuz is shown. Upper portion of the Strait is covered by clouds. An ocean thermal feature appears in the upper Gulf of Oman. $2^{\circ}x2^{\circ}$ grid spacing.

Figure 6. Gulf of Oman.

The Gulf of Oman is shown from the Strait of Hormuz to Ra's al Hadd. Muscat is in the center and Iran is in the upper portion. In addition to features in the upper Gulf, a large cyclonic eddy appears between Muscat and Ra's al Hadd. $2^{\circ}x2^{\circ}$ grid spacing. The position of Muscat is $23^{\circ}35'N$, $58^{\circ}30'E$. The location of Ra's al Hadd is $22^{\circ}25'N$, $59^{\circ}50'E$. The nearest grid intersection to the Strait of Hormuz is $26^{\circ}N$, $56^{\circ}E$.

Figure 7. Gulf of Oman.

The outer Gulf of Oman is shown just east of that of Figure 6. The image is dominated by clouds in the upper right portion. The ocean feature on the extreme left is the same feature seen in Figure 6. A warm intrusion separates the cold eddy in the lower left hand corner from a series of cold eddies in the lower left region. $2^{\circ}x2^{\circ}$ grid spacing. The grid intersection in the upper left corner is $24^{\circ}N$, $60^{\circ}E$ and is common to both Figures 6 and 7.

Figure 8. Coastal Region South of Gulf of Oman.

The coastal region is shown southeast of the Island of Masirah. An ocean feature dominates the center of the image and appears to emanate from the south tip of the island. This feature lies to the north of a warm anticyclonic eddy and is capped by a cold cyclonic eddy outlined by a warm intrusion in the upper right portion. The upwelling south of the Island of Masirah is cold enough to saturate the white in the image. $2^{\circ}x2^{\circ}$ grid spacing. The southern tip of Masirah Island is at $20^{\circ}15'N$, $58^{\circ}40'E$, and the nearest grid intersection is $20^{\circ}N$, $58^{\circ}E$.

Figure 9. Coastal Region Off Arabian Peninsula.

The coastal region is shown from Ra's Madrakah to Ra's Mirbat. A large group of features dominates the field of view with cyclonic cold eddies and anticyclonic warm eddies outlined by cold features. Upwelling appears south of Ra's Madrakah. $2^{\circ}x2^{\circ}$ grid spacing. Ra's Madrakah in the top center is at $19^{\circ}0'N$, $57^{\circ}50'E$, with the nearest grid intersection at $18^{\circ}N$, $60^{\circ}E$.

Figure 10. Coastal Region Off Arabian Peninsula.

The coastal region is shown from Ra's Mirbat to Ra's Fartak. The Island of Socotra appears in the lower center of the image. Ocean thermal features are seen filling the entrance to the Gulf of Aden between Socotra Island and Ra's Fartak and beyond to Ra's Mirbat. $2^{\circ}x2^{\circ}$ grid spacing. The eastern tip of Socotra Island is at $12^{\circ}30'N$, $54^{\circ}30'E$. Ra's Mirbat is at $17^{\circ}15'N$, $55^{\circ}20'E$ and Ra's Fartak is at $15^{\circ}35'N$, $52^{\circ}15'E$.

Figure 11. Gulf of Aden.

The entrance to the Gulf of Aden is shown between the Horn of Africa and the coast of the Arabian Peninsula. A faint tip of the western point of the Island of Socotra appears in the extreme right. Ocean thermal features dominate this region between the coast of the Arabian Peninsula, the Horn of Africa, and the Island of Socotra. $2^{\circ}x2^{\circ}$ grid spacing. The tip of the Horn of Africa (Ra's Aser) is at $11^{\circ}45'N$, $51^{\circ}20'E$.

Figure 12. Ocean Region Near Horn of Africa.

The ocean region to the east and southeast of the Horn of Africa is shown. The Island of Socotra appears in the upper left. Clouds overlie portions of the view but weak thermal features to the southeast of Socotra Island suggest the demise of the Southwest Monsoon. $2^{\circ}x2^{\circ}$ grid spacing. The east tip of Socotra Island is at $12^{\circ}30'N$, $54^{\circ}30'E$.

Figure 13. Ocean Region East of Socotra Island.

The next adjacent region of the ocean east of Figure 12 is shown. The cloud pattern in the left portion is the cloud pattern seen in the right portion of Figure 12. Some extension of ocean features seen in Figure 12 can be followed through the cloud patterns. $2^{\circ}x2^{\circ}$ grid spacing.

Figure 14. Western Portion of Upper Arabian Sea.

A region east of Ra's Fartak and south of Ra's al Hadd is shown. This view shows the continuation of the ocean thermal feature south of the feature in Figure 8 and east of the feature shown in Figure 9. $2^{\circ}x2^{\circ}$ grid spacing. The feature lies along $16^{\circ}N$, mostly between $60^{\circ}E$ and $62^{\circ}E$. It bifurcates east of $62^{\circ}E$.

Figure 15. Persian Gulf.

The interpretation is shown for the ocean thermal feature which appears in Figure 4. A weak (wk) front is shown surrounding the feature. The legend indicates NOAA-6, 1980, Julian 300, enhanced image number two.

Figure 16. Strait of Hormuz.

The interpretation is shown for the image in Figure 5. Both strong (stg) and weak (wk) ocean fronts are indicated with clouds (clds) overlying the strait. The legend indicates NOAA-6, 1980, Julian 300, enhanced image number one.

Figure 17. Gulf of Oman.

The interpretation is shown for the image in Figure 6. The shallow features in Figure 16 show in the upper left portion of this figure. Both strong (stg) and weak (wk) ocean fronts are indicated as well as ocean eddies. Clouds (clds) overlie much of the land and a portion of the right center image. A large cyclonic cold eddy is seen in the Gulf of Oman between Muscat and Ra's al Hadd which is affected near shore by light winds directed by the mountains between Muscat and Ra's al Hadd. The legend indicates NOAA-6, 1980, Julian 300, enhanced image number three.

Figure 18. Gulf of Oman.

The interpretation is shown for the image in Figure 7. Several weak (wk) ocean fronts are indicated in the region not covered by clouds (clds). The edge of a cold cyclonic eddy appears in the left portion which also appears in the right portion of Figure 17. A warm intrusion is indicated in the lower left between a cold eddy in the extreme lower left and several eddies near the middle of the lower left. The legend indicates NOAA-6, 1980, Julian 300, enhanced image number four.

Figure 19. Coastal Region South of Gulf of Oman.

The interpretation is shown for the image in Figure 8. A strong (stg) flow is indicated associated with a major feature which propagates from upwelling off the south tip of the Island of Masirah. A cold cyclonic eddy is indicated to the north of this tongue-like feature. A sequence of warm and cold eddies is indicated in progression down the coast of the Arabian Peninsula, and major features associated with points of land are repeated along the coast. The legend indicates NOAA-6, 1980, Julian 300, enhanced image number five.

Figure 20. Coastal Region Off Arabian Peninsula.

The interpretation is shown for the image in Figure 9. Both strong (stg) and weak (wk) ocean fronts are indicated. There is a continuation of warm eddies surrounded by cold features in this progression down the coast of the Arabian Peninsula. A small cold cyclonic eddy is indicated near the center of the image. The legend indicates NOAA-6, 1980, Julian 300, enhanced image number six.

Figure 21. Coastal Region Off Arabian Peninsula.

The interpretation is shown for the image in Figure 10. Upwelling is apparent north and to the sides of the Island of Socotra. A large anticyclonic eddy is indicated in the eddy field north of the island. Several weak (wk) ocean fronts

are indicated. This image shows the setup of the eddy field in the entrance to the Gulf of Aden between Socotra and the Arabian Peninsula. Slicking in the lower right portion of the image is an indication of surface daytime heating which has not been mixed in the absence of winds. The legend indicates NOAA-6, 1980, Julian 300, enhanced image number seven.

Figure 22. Gulf of Aden.

The interpretation is shown for the image in Figure 11. A continuation of the thermal structure and eddy field at the entrance to the Gulf of Aden is shown in this image progressing into the gulf. There is upwelling off the Horn of Africa and longshore flow near the coast of the Arabian Peninsula. Both strong (stg) and weak (wk) ocean fronts are indicated. The legend indicates NOAA-6, 1980, Julian 300, enhanced image number eight.

Figure 23. Ocean Region Near Horn of Africa.

The interpretation is shown for the image in Figure 12. The nature of the clouds (clds) is indicative of light winds in the area. In addition to the upwelling and strong (stg) frontal features associated with the Island of Socotra, the ocean thermal field is dominated by slicking patterns. The slicking, caused by daytime heating, has remained on the surface due to the absence of winds. These slicking patterns tend to outline the relative surface flow. The legend indicates NOAA-6, 1980, Julian 300, enhanced image number nine.

Figure 24. Ocean Region East of Socotra Island.

The interpretation is shown for the image in Figure 13. A continuation of the clouds (clds) and interpretive features in Figure 23 can be seen in this image which lies to the east of the area in Figure 23. The legend indicates NOAA-6, 1980, Julian 300, enhanced image number ten.

Figure 25. Western Portion of Upper Arabian Sea.

The interpretation is shown for the image in Figure 14. Substantial thermal structure is indicated in this image. This structure is the extension of structures closer to the Arabian Coast identified in Figures 19 and 20. The legend indicates NOAA-6, 1980, Julian 300, enhanced image number thirteen.

Figure 26. Arabian Sea Infrared Image Mosaic, 28 March 1980.

A composite of enhanced images is shown with the Gulf of Oman and the coasts of Iran and Pakistan at the top, and the Arabian Peninsula coast on the left. Clouds appear in the lower right. Ocean thermal features dominate all of the view of the ocean surface. A separate low resolution satellite view from Channel Three of the NOAA-6 satellite appears left of the mosaic and indicates the data from which the composite was made.

Figure 27. Arabian Sea Infrared Image Mosaic, 15 April 1980.

A composite of enhanced images is shown with the Gulf of Oman and coast of Iran at the top, and the Arabian Peninsula coast on the left. There are clouds in the lower right. Ocean thermal features appear over most of the view of the ocean surface. A separate low resolution satellite view from Channel Three of NOAA-6 appears left of the mosaic and indicates the data from which the composite was made.

Figure 28. Arabian Sea Infrared Image Mosaic, 21 May 1980.

A composite of enhanced images is shown with the Persian Gulf, Strait of Hormuz, Gulf of Oman, and coast of Iran at the top, and the Arabian Peninsula coast on the left. Cloud bands dominate the ocean view and illustrate the beginning of the summer Southwest Monsoon. Ocean thermal features can be seen where the ocean surface is exposed. A separate low resolution satellite view from Channel Three of NOAA-6 appears right of the mosaic and indicates the data from which the composite was made.

Figure 29. Arabian Sea Infrared Image Mosaic, 30 May 1980.

A composite of enhanced images is shown with the lower Persian Gulf, Strait of Hormuz, Gulf of Oman, and coast of Iran at the top, and the Arabian Peninsula coast on the left. The entrance to the Gulf of Aden can be seen as well as portions of the Island of Socotra. Clouds appear to dominate much of the ocean view. Strong ocean thermal features can be seen wherever the ocean surface is exposed, such as along the coast and in the Gulf of Oman. A separate low resolution satellite view from Channel Three of NOAA-6 appears left of the mosaic and indicates the data from which the composite was made.

Figure 30. Arabian Sea Infrared Image Mosaic, 28 September 1980.

A composite of enhanced images is shown with the Persian Gulf, Strait of Hormuz, Gulf of Oman, and coast of Iran at the top, and the Arabian Peninsula coast on the left. Clouds cover most of the Arabian Sea but ocean thermal features can be seen where the ocean surface is exposed. A separate low resolution satellite view from Channel Three of NOAA-6 appears left of the mosaic and indicates the data from which the composite was made.

Figure 31. Arabian Sea Infrared Image Mosaic, 30 September 1980.

A composite of enhanced images is shown with the lower Persian Gulf, Strait of Hormuz, Gulf of Oman, and coast of Iran at the top, and the Arabian Peninsula coast on the left. Clouds appear on the lower portion. Strong ocean thermal features can be seen where the ocean surface is exposed. A separate low resolution satellite view from Channel Three of NOAA-6 appears left of the mosaic and indicates the data from which the composite was made.

Figure 32. Arabian Sea Infrared Image Mosaic, 26 October 1980.

A composite of enhanced images is shown with the lower Persian Gulf and Gulf of Oman at the top, and the Arabian Peninsula coast on the left. Clouds appear in the upper right and lower portions of the mosaic. Strong ocean thermal features can be seen wherever the ocean surface is exposed. A separate low resolution satellite view from Channel Three of NOAA-6 appears left of the mosaic and indicates the data from which the composite was made.

Figure 33. Arabian Sea Infrared Image Mosaic, 25 November 1980.

A limited composite of enhanced images is shown with the Strait of Hormuz, coast of Iran, and Gulf of Oman at the top, and a portion of the Arabian Peninsula coast in the left center. The Island of Masirah appears in the lower portion. Clouds appear on the right and weak ocean thermal features can be seen between the clouds and the Arabian Peninsula. A separate low resolution satellite view from Channel Three of NOAA-6 appears left of the mosaic and indicates the data

from which the composite was made. The composite was limited due to masking by atmospheric moisture and absence of apparent ocean thermal structure in regions farther down the Arabian Coast.

Figure 34. Arabian Sea Infrared Image Mosaic, 27 November 1980.

A composite of enhanced images is shown with the Strait of Hormuz, coast of Iran, and Gulf of Oman at the top, and the Arabian Peninsula coast on the left. Clouds dominate much of the field of view and weak ocean thermal features can be seen near the coast, becoming stronger in the Gulf of Aden. A separate low resolution satellite view from Channel Three of NOAA-6 appears left of the mosaic and indicates the data from which the composite was made.

Figure 35. Arabian Sea Infrared Image Mosaic, 30 November 1980.

A composite of enhanced images is shown with the Strait of Hormuz and Gulf of Oman at the top and the Arabian Peninsula on the left. Clouds cover most of the Arabian Sea but some ocean thermal features can be seen where the ocean is exposed along the Arabian coast. A separate low resolution satellite view from Channel Three of NOAA-6 appears left of the mosaic and indicates the data from which the composite was made.

Figure 36. Arabian Sea Mosaic with Interpretation, 28 March 1980.

The composite of enhanced images shown in Figure 26 is shown here with a composite of surface interpretations for each image. Relative flow is indicated by arrows, and strong and weak fronts are indicated by solid and dashed lines respectively. Shear flow is indicated by a row of "x's". Slicking from daytime heating appears where there has been little surface mixing.

Figure 37. Arabian Sea Mosaic with Interpretation, 15 April 1980.

The composite of enhanced images shown in Figure 27 is shown here with a composite of surface interpretations for each image. Relative flow is indicated by arrows, and strong and weak fronts are indicated by solid and dashed lines respectively. (A poor alignment of lines indicating fronts occurred in the printing process.)

Figure 38. Arabian Sea Mosaic with Interpretation, 21 May 1980.

The composite of enhanced images shown in Figure 28 is shown here with a composite of surface interpretations for each image. Relative flow is indicated by arrows, and strong and weak fronts are indicated by solid and dashed lines respectively. Shear flow is indicated by a row of "x's". Upwelling regions are designated.

Figure 39. Arabian Sea Mosaic with Interpretation, 30 May 1980.

The composite of enhanced images shown in Figure 29 is shown here with a composite of surface interpretations for each image. Relative flow is indicated by arrows, and strong and weak fronts are indicated by solid and dashed lines respectively. Shear flow is indicated by a row of "x's". Upwelling is designated. (A poor alignment of lines indicating fronts occurred in the printing process.)

Figure 40. Arabian Sea Mosaic with Interpretation, 28 September 1980.

The composite of enhanced images shown in Figure 30 is shown here with a composite of surface interpretations for each image. Relative flow is indicated by arrows, and strong and weak fronts are indicated by solid and dashed lines respectively.

Figure 41. Arabian Sea Mosaic with Interpretation, 30 September 1980.

The composite of enhanced images shown in Figure 31 is shown here with a composite of surface interpretations for each image. Relative flow is indicated by arrows, and strong and weak fronts are indicated by solid and dashed lines respectively.

Figure 42. Arabian Sea Mosaic with Interpretation, 26 October 1980.

The composite of enhanced images shown in Figure 32 is shown here with a composite of surface interpretations for each image. Relative flow is indicated by arrows, and strong and weak fronts are indicated by solid and dashed lines respectively. The interpretations in this mosaic are described in more detail in Figures 15 through 25.

Figure 43. Arabian Sea Mosaic with Interpretation, 25 November 1980.

The composite of enhanced images shown in Figure 33 is shown here with a composite of surface interpretations for each image. Only weak surface features are indicated.

Figure 44. Arabian Sea Mosaic with Interpretation, 27 November 1980.

The composite of enhanced images shown in Figure 34 is shown here with a composite of surface interpretations for each image. Clouds dominate the field of view with some weak thermal features indicated on the ocean surface.

Figure 45. Arabian Sea Mosaic with Interpretation, 30 November 1980.

The composite of enhanced images shown in Figure 35 is shown here with a composite of surface interpretations for each image. Relative flow is indicated by arrows, and strong and weak fronts are indicated by solid and dashed lines respectively. (A poor alignment of lines indicating fronts occurred in the printing process.)

INTRODUCTION

This is the second in a series of three reports concerning infrared imagery of the Arabian Sea. The first report (ONRWEST Report 81-3) described a technique which was developed to produce and interpret infrared imagery. These data were obtained from the NOAA-6 satellite tape recorder during passes over the Arabian Sea in 1980. This report presents a substantial portion of the infrared imagery obtained in 1980. A third report is planned which will present detailed images concerning selected features in the northwestern portion of the Arabian Sea.

Mesoscale structures of the Arabian Sea are apparent during all seasons of the year, and are dominated by upwelling-derived plumes and wedges of cold water extending seaward from the Arabian coast. These features may separate and sometimes circumscribe ocean eddies. Warm- and cold-core eddies occur throughout the upper portions of the Arabian Sea. Mesoscale features are forced by the meteorological conditions of the winter and summer monsoonal winds and positioned by coastal topography and points of land. Sufficient data are presented in this report to illustrate the spring transition from winter to summer monsoonal flows and the fall transition from summer to winter monsoonal flows. From these transitions, the major characteristics of the summer and winter ocean structures can be determined.

As yet, there are few ground-truth data from the Arabian Sea to support the interpretations for the mesoscale features highlighted in these infrared images. Much of the interpretation is based on experience with similar features observed near coastlines in other parts of the world's oceans where mesoscale structures are known to be deep and bounded by strong horizontal thermal gradients. Thus, the assumption is made that the data presented in this report are indicative of the dominant mesoscale structures of the Arabian Sea.

TECHNIQUE

The technique for enhancing and interpreting infrared imagery is described in a previous report (ONRWEST Report 81-3). All infrared images presented in this report were obtained by photographing the cathode ray tube (CRT) of a high resolution television set by means of a 35mm camera. Each image has been enhanced and studied in great detail using the various interpretive routines available in the computer software of the Scripps Institution of Oceanography Remote Sensing Facility (SRSF). After examining all of the subtle implications of the features seen, a compromise of temperature scales and range of grey shades was set on the CRT for the purpose of photography. Thus, the photographs presented in this report are indicative of the thermal features seen on the CRT and the interpretations presented in this report are indicative of the interpretations made at the time of image enhancement and analysis.

Large prints were made from the photography, and matching large transparencies were made for the interpretations. Composite arrangements (mosaic patterns) of these images were used in explaining the mesoscale features of the Arabian Sea to various operational and research audiences before preparing the photographically reduced figures for this report. Loss of the finer details of the mesoscale features occurred in the preparation and reproduction processes necessary to make the figures. In addition, transparent overlays could not be reproduced for this report so the figures containing interpretations were made by photographing the overlay superimposed on the image without interpretation. Unfortunately, some mismatch of interpretive lines and ocean features occurred in the process.

The Advanced Very High Resolution Radiometer (AVHRR) on board the National Oceanic and Atmospheric Administration's satellite (NOAA-6) has five channels in spectral bands from 0.55 μm to 12.5 μm. Channel Three records at 3.55 μm to 3.93 μm. Channels Four and Five record at 10.5 μm to 11.5 μm, and 11.5 μm to 12.5 μm respectively. All channels have a data resolution of one-half nautical mile (1.1 km) at the satellite subpoint. Although there is less atmospheric contamination in tropical regions at the 3.55 μm to 3.93 μm band than at the other bands, Channel Three unfortunately suffers from instrument noise which has become worse with time. It appears to be no better on the new NOAA-7 satellite. Because the noise is linear, much of it can be removed by averaging and matching routines available in the computer software. All data in this report were obtained from Channel Three.

DATA COMPONENTS

Individual enhanced infrared images are derived from the satellite view recorded on 26 October 1980 (Figures 4-25). Each enhanced image was of a field of view of 512x512 pixels. The images have been clipped in the reproduction process so that the field of view is closer to 500x500 km. The low resolution image in Figure 3, obtained from Channel Three of the NOAA-6 satellite, illustrates the source of data for these enhanced images. Each one is a component of the low resolution view and subdivides that view into regions primarily along the coast of the Arabian Peninsula.

The interpretations in Figures 15 through 25 were prepared as overlays on the enhanced images (Figures 4-14). Because the satellite records a synoptic view, or snapshot, of the general structure and flow pattern on the surface of the ocean, it provides only the relative instantaneous motion of the water. Thus, the interpretations, indicated by arrows, are intended to illustrate the sense of motion in mesoscale features, not the general flow of the ocean.

Strong horizontal thermal gradients in surface features, obtained by analysis in the SRSF, were used to determine strong ocean fronts. These are indicated by solid lines in the interpretations. Likewise, weak thermal gradients indicative of weaker fronts are indicated by dashed lines. Some intuition about the relative motion between mesoscale features, as well as clues from small wisp-like vortices (visible only on the original enhanced image), have been used to determine shear flow in some regions of the mesoscale flow field. This shear flow is indicated by a series of "x's" marked along the line of shear.

Athough warm- and cold-core eddies can be distinguished in the mesoscale features in these images, they have not been labeled so in the interpretations. A cold-core eddy rotates cyclonically (counterclockwise) and a warm-core eddy rotates anticyclonically (clockwise). Such patterns can be seen. Some of the circular patterns appear to rotate in the opposite sense. For example, a plume of cold upwelled water may extend and partially circumscribe a warm-core eddy in a fashion as to make it appear that the eddy is rotating cyclonically. Again, warm intrusions can be seen to surround some of the cold-core eddies to give the impression that the eddy is rotating anticyclonically. Because of these apparent effects and the lack of ground-truth data, the direction of rotation indicated in the interpretations of some of these features could be wrong. The primary purpose here is to present the mesoscale thermal features in a relative sense and to indicate the general speculations made from those observed features.

The component-enhanced images obtained for the satellite view recorded on 26 October 1980 are presented in this report as an example of the components available from all of the recorded satellite views. A complete list of satellite views stored on tapes at SRSF is given in ONRWEST Report 81-3. These components were used to form the composites (Figures 26-45).

DATA COMPOSITES

Each enhanced image, presented as a component of the satellite view obtained on 26 October 1980, is presented without the overlay interpretation in Figures 4 through 14. These components are then arranged in a mosaic pattern comparable to the image in Figure 3 but made up of enhanced images to illustrate a greatly magnified view. This mosaic arrangement is presented as a composite of enhanced images in Figure 32. The composite does not form a perfect mosaic because the view near the edges of each enhanced image is slightly distorted and, therefore, distorted features match poorly across boundaries of components in the mosaic.

The enhancement photographed for each image was a compromise on the range of temperatures in that field of view. There are substantial temperature differences from the Gulf of Oman to the Gulf of Aden, so that the enhancement varied for each component image progressing down the Arabian Coast. An attempt was made to center the grey shades on the middle temperature of each enhanced image. This technique made it unlikely that the grey shades would match at the boundaries of printed images. Thus, the cut lines in adjacent components of the mosaic appear to be the dominant steps in grey shades in each composite, as in Figure 32; such artifacts of the mosaic process are ignored in following the ocean thermal features across component boundaries.

The components in the composite of Figure 32 have computer-drawn grid lines which approximate 2^{o} increments in latitude and longitude. These grid lines can be located by reference to Figure 2 which provides the tabular listing of locations and nearest intersections. Again, these grid lines do not match perfectly across component boundaries because of the distortions near the edges of the view in each image.

The low resolution infrared image representing the satellite view presented in Figure 3 is repeated in Figure 32 to illustrate the data from which the composite was derived. The grid lines in this low resolution image have a 5^{o} spacing.

The composites of enhanced images obtained on ten representative days in 1980 are presented in Figures 26-35. In each case the composite was produced in a manner similar to that of Figure 32. Some of these composites lack the 2^{o} grid pattern and the satellite view lacks the 5^{o} grid pattern because the earth location could not always be obtained from the tapes. All composite figures are presented on approximately the same spatial scale, so that geographical locations of features can be approximated by comparison with those illustrations that are grided.

Some details in the field of view of each composite are highlighted in the abbreviated paragraph following the title on each figure. In general, identifying coastal references can be determined and the mesoscale structures of the ocean can be seen wherever the field of view is not contaminated by clouds. White is used to indicate colder water and black is used to indicate warmer water. The enhancement process assigns land and clouds, which are always much warmer or colder than the ocean mesoscale features, to either black or white, because only the coastal silhouette and clouds need be distinguished in the interpretation of ocean thermal structures.

The NOAA-6 satellite passes in the early evening, local time, and the effect of residual daytime heating on the land appears black (warm) in most of the composites. Clouds over land and some portions of the land appear to be white. White portions of land in springtime and fall correlate with regions of sand which undergo rapid surface cooling after sunset. Since sunset occurs earlier in the fall, more of the land is white because it has had time to cool. These image composites in Figures 26 through 35 were originally made on large, black posterboards for use in lectures. Photographic reduction for the figures in this report caused some loss in detail but still preserves the essence of the mesoscale features.

The enhanced image composites of Figures 26 through 35 are repeated in Figures 36 through 45 with the addition of the overlaid interpretations. Just as in the process of making mosaic patterns of enhanced images, the overlays were pieced together to match the composites of images. Again, there were some mismatches at the boundaries of the components. The component transparent overlays were originally made to be used with the individual enhanced images, so these overlays possess portions of distinguishing labels which have not been entirely removed in forming the mosaic.

The process of producing the interpretations described previously for Figures 15 through 25 apply to these composites of interpretations presented in Figures 36 through 45. The sense of the relative instantaneous flow patterns seen in the infrared image is indicated by arrows. Strong and weak thermal fronts are indicated by solid and dashed lines. Regions of shear are indicated by a line of "x's" and upwelling is designated where it is a dominant feature. The abbreviated paragraph which follows the title of each figure highlights some major aspects of the interpretations. Figures 36 through 45 were made by overlaying the mosaics of transparent interpretations of individual components for Figures 26 through 35, and some overlays were shifted slightly in the process so that the lines do not overlie perfectly the boundaries between lighter and darker grey shades.

SEASONAL GUIDELINES

Because of satellite scheduling problems, it was not possible to obtain satellite infrared imagery data at the height of the winter Northeast Monsoon or the summer Southwest Monsoon. Sufficient data were obtained, however, to identify the spring and fall transitions between monsoonal seasons. The data presented for the period from late March to late May indicate the final stage of the winter monsoon and the onset of the summer monsoon. Likewise, the data presented for the period from late September to the end of November indicate the remnants of the summer monsoon and the beginning of the winter monsoon. From these transitions, the major mesoscale features of the ocean during the height of each monsoonal season can be inferred.

Some upwelling is apparent from the very beginning of the spring transition period. The effects of the Southwest Monsoon are demonstrated in a continual strengthening of the upwelling along the coast of the Arabian Peninsula. Upwelling features are associated with points of land and relatively shallow regions such as around Masirah Island. Upwelling also occurs around Socotra Island. Cold plumes and wedges form from these upwelling regions and extend offshore. These colder tongues are drawn offshore and tend to outline the regions of warmer and colder ocean eddies. The spring transition is the time of strengthening and stabilizing the mesoscale structures which will be dominant during the Southwest Monsoon. The summer season is then inferred to be a time of strong upwelling plumes and wedges delineating relatively strong warm- and cold-core eddies which fill most of the northwestern Arabian Sea from the Horn of Africa to the Gulf of Oman.

It is known from many sources that strong winds and high seas dominate much of the Arabian Sea during summer. Wind speeds may be persistent between 25 and 35 knots with gusts reaching 40 to 45 knots. The winds blow over a long fetch from south of the Equator, so that large swell occur topped with large wind waves--creating a formidable sea. The resultant mixing of near surface waters may smear the surface indications of thermal structures but the structures themselves are strong and relatively deep.

The summer Southwest Monsoon ends with a shifting and dying windfield that leaves a great deal of moisture and clouds in the atmosphere. Upwelling along the coast of the Arabian Peninsula does not cease abruptly but continues well into the fall season. There is some appearance of "backing and turning" of the cold plumes and wedges which emanated from regions of strong upwelling. The procession of warm- and cold-core eddies may move relatively little as seen in comparing the composite images for 28 and 30 September. Tongue-like cold-water wedges which extended from the coast between Masirah Island and Ra's al Hadd move up and down the coast between these points, sometimes splitting into two features. Where one strong feature may dominate during the height of the Southwest Monsoon, complex patterns of these features are encountered following the diminishing of the winds. Mixing and dissipation of the strong thermal features generated during summer takes place slowly in the fall. Consequently, strong thermal features can be expected through October, even though their locations may not be as easily designated by reference to points of land.

The ocean thermal features have weakened by the latter part of November but some "backing and filling" of the remnants of the transition can still be associated with topographic features along the coast of the Arabian Peninsula.

Strong features which fill the entrance to the Gulf of Aden may persist throughout the spring and fall transition periods.

The winter Northeast Monsoon provides a season of mild winds and relatively dry atmosphere. These benign meteorological conditions permit the dying of coastal upwelling and associated cold features offshore. Regions of warm- and cold-core eddies are still apparent and probably persist throughout the winter until the first stages of the spring transition.

CONCLUSIONS

The Arabian Sea is dominated by mesoscale structures that form thermal patterns which can be identified by satellite-derived infrared images. These mesoscale structures are primarily warm- and cold-core eddies with cold-water plumes and wedges partially circumscribing the eddies, and with some warm-water intrusions separating the eddies.

The dominant forces that create the mesoscale structures are the winds of the summer Southwest Monsoon and the winter Northeast Monsoon. Positions of the features in the northwestern Arabian Sea can be associated with the general topography of the coastline and points of land.

Upwelling occurs throughout most of the year along the coast of the Arabian Peninsula and can be identified and monitored by satellite infrared imagery. The extent and movement of upwelled waters can be analyzed if successive days of satellite imagery are available to discern the patterns of the changing mesoscale features.

The depth of the mesoscale structures in the Arabian Sea has not been determined by direct measurements. The impression that these features are relatively deep has been inferred by experience with mesoscale features in other oceans.

FIGURES

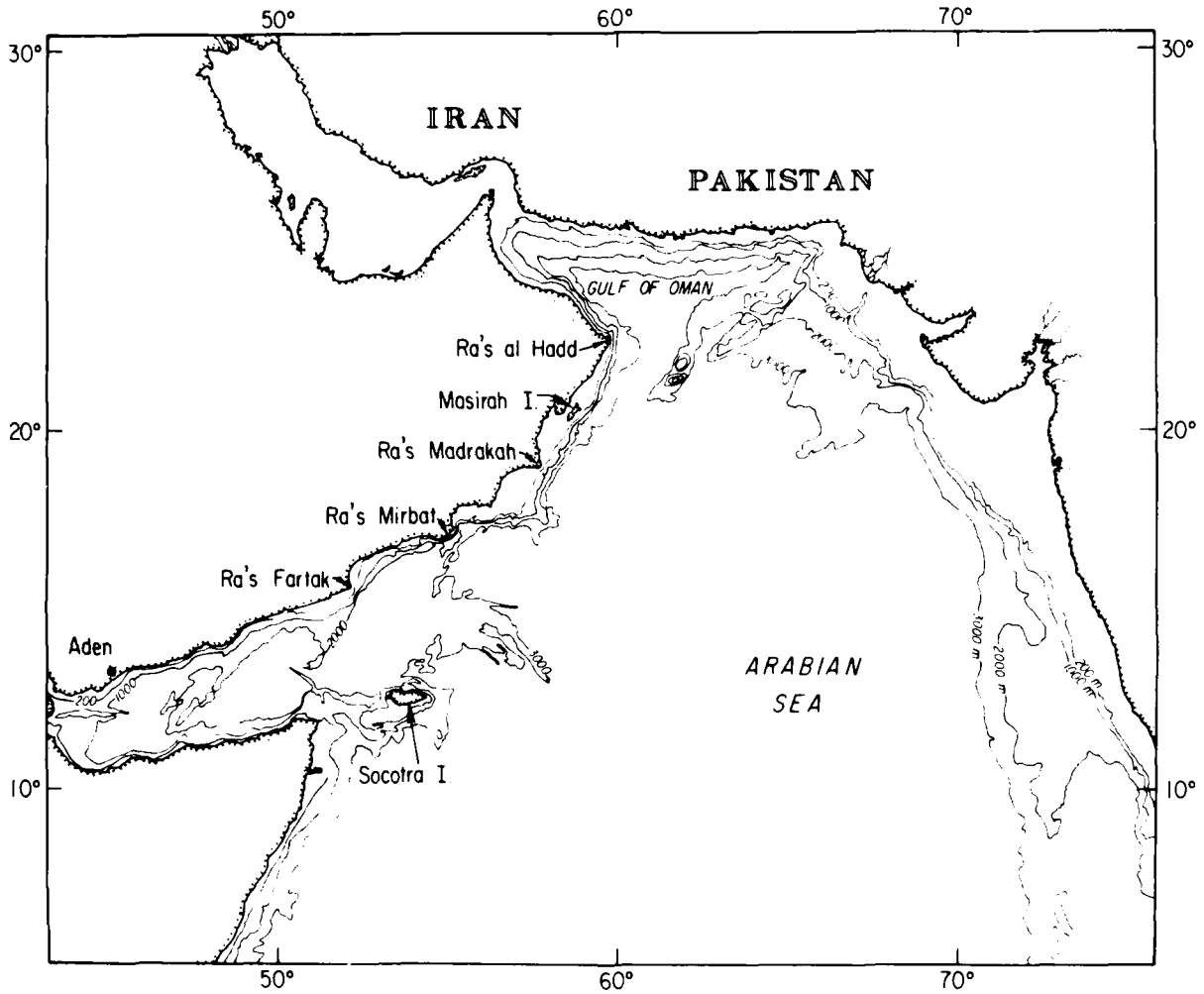

Figure 1. Map of Arabian Sea.

The Arabian Sea is bounded on the west by the Arabian Peninsula, on the north by the coasts of Iran and Pakistan, and on the east by the coast of India. Bathymetry is provided down to 3000 meters to illustrate the rapid falloff of the shelf in some areas. The Oman Basin is partially closed by the Murray Ridge with an opening to the Arabian Sea near the Arabian Coast.

TOPOGRAPHICAL REFERENCE POINTS

Identity	Position	Nearest Intersection on Images
(Coastal)		
Muscat	23°35'N, 58°30'E	24°N, 58°E
Ra's al Hadd	22°25'N, 59°50'E	22°N, 60°E
Masirah Island (Southern Tip of Island)	20°15'N, 58°40'E	20°N, 58°E
Ra's Madrakah	19°0'N, 57°50'E	18°N, 58°E
Ra's Mirbat (Ra's Naws) (Easternmost Extension of Land)	17°15'N, 55°20'E	18°N, 56°E
Ra's Fartak	15°35'N, 52°15'E	16°N, 52°E
Horn of Africa (Tip) (Ra's Aser)	11°45'N, 51°20'E	12°N, 52°E
Socotra Island (Eastern Tip of Island)	12°30'N, 54°30'E	12°N, 54°E
(Ocean Bottom)		
Murray Ridge (Orientation NE-SW) (At the 3000m Depth Line)	From: 24°25'N, 65°30'E (NE) To: 20°45'N, 61°0'E (SW)	

Figure 2. Points of Reference.

These points of reference are used to identify possible topographic effects and to give location to features in the infrared images.

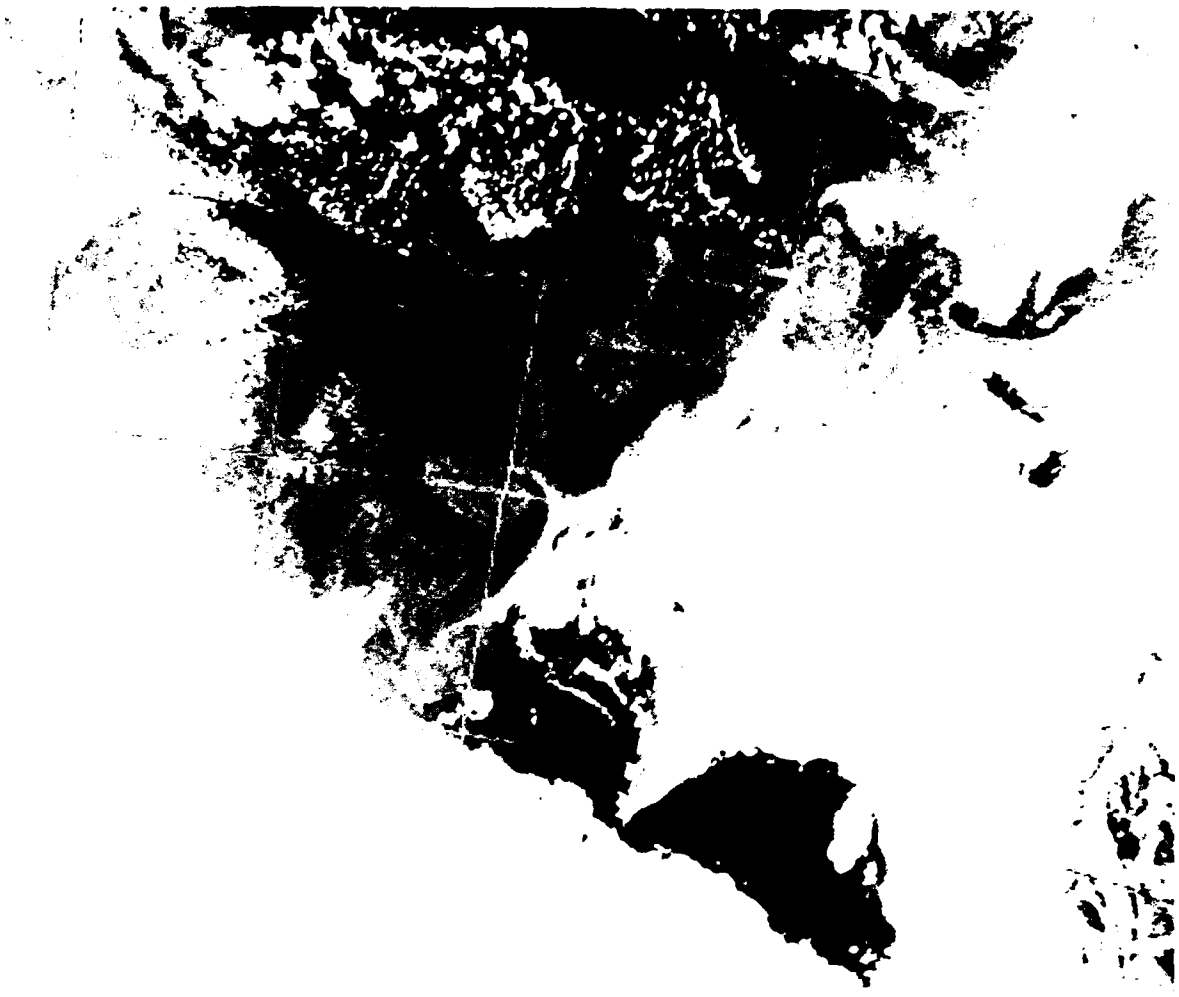

Figure 3. Satellite Infrared Image of the Arabian Sea.

This is a low resolution, infrared image obtained from Channel Three of the NOAA-6 satellite on 26 October 1980 (Julian day 300). An ocean thermal feature appears in the center of the view. Both white and black in the image represent saturated data. Clouds appear in the lower and right hand portions of the image. $5^{o}x5^{o}$ grid spacing.

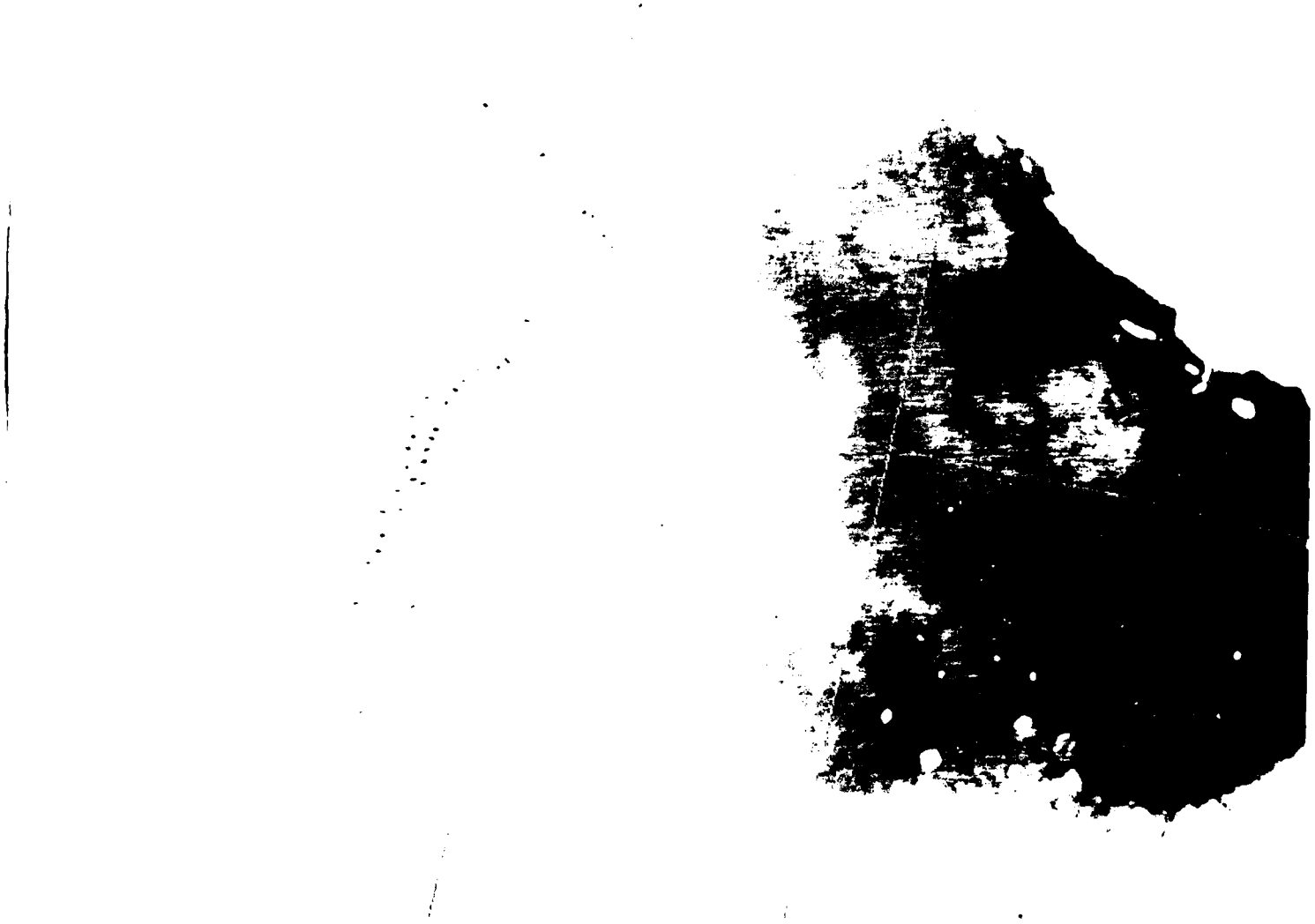

Figure 4. Persian Gulf.

The lower portion of the Persian Gulf is shown from the vicinity of Qatar to Abu Dhabi. A faint ocean thermal feature appears in the center. The white is saturated data, especially west of Qatar. $2^{o}x2^{o}$ grid spacing.

Figure 5. Strait of Hormuz.

The vicinity on both sides of the Strait of Hormuz is shown. Upper portion of the Strait is covered by clouds. An ocean thermal feature appears in the upper Gulf of Oman. $2^{o}x2^{o}$ grid spacing.

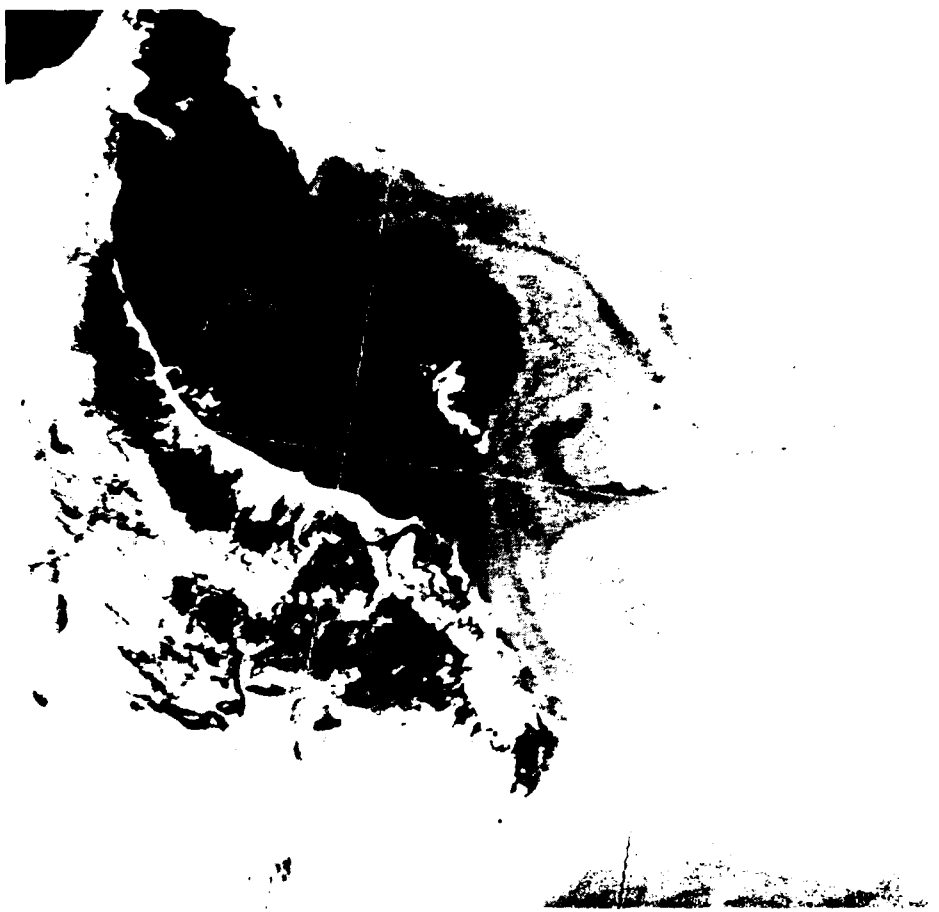

Figure 6. Gulf of Oman.

The Gulf of Oman is shown from the Strait of Hormuz to Ra's al Hadd. Muscat is in the center and Iran is in the upper portion. In addition to features in the upper Gulf, a large cyclonic eddy appears between Muscat and Ra's al Hadd. $2^{o}x2^{o}$ grid spacing. The position of Muscat is $23^{o}35'N$, $58^{o}30'E$. The location of Ra's al Hadd is $22^{o}25'N$, $59^{o}50'E$. The nearest grid intersection to the Strait of Hormuz is $26^{o}N$, $56^{o}E$.

Figure 7. Gulf of Oman.

The outer Gulf of Oman is shown just east of that of Figure 6. The image is dominated by clouds in the upper right portion. The ocean feature on the extreme left is the same feature seen in Figure 6. A warm intrusion separates the cold eddy in the lower left hand corner from a series of cold eddies in the lower left region. $2^{o}x2^{o}$ grid spacing. The grid intersection in the upper left corner is $24^{o}N$, $60^{o}E$ and is common to both Figures 6 and 7.

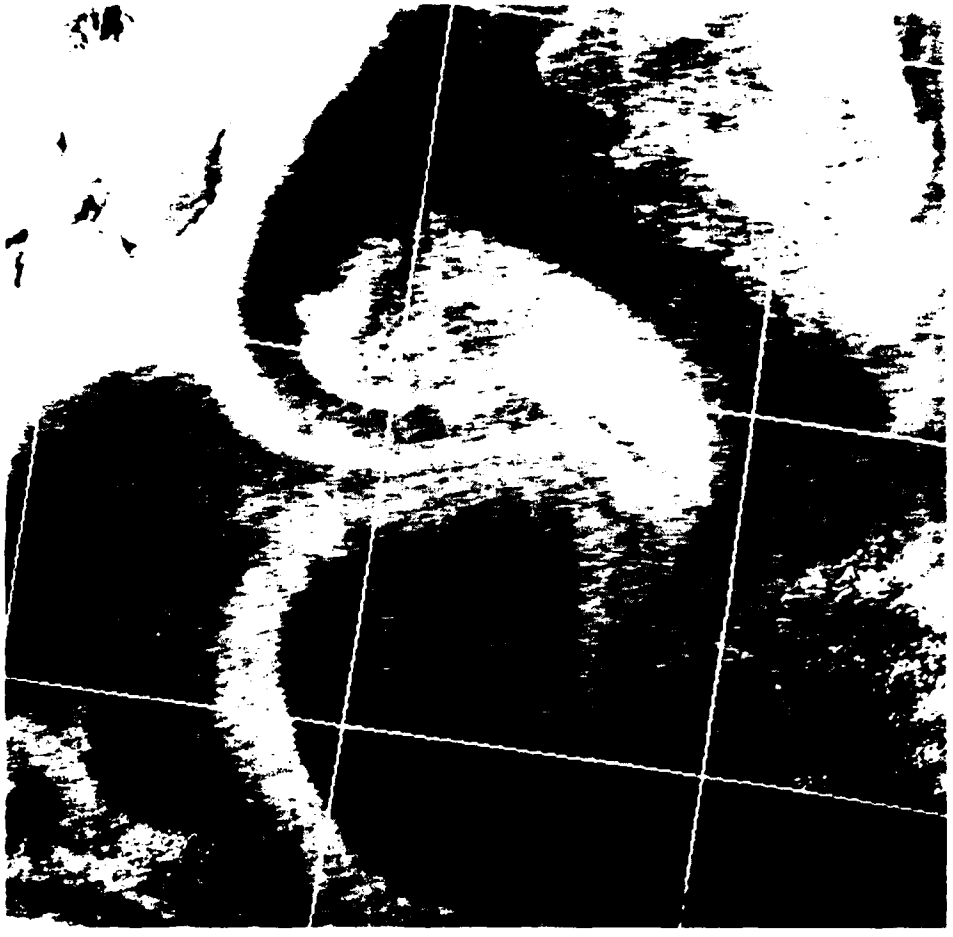

Figure 8. Coastal Region South of Gulf of Oman.

The coastal region is shown southeast of the Island of Masirah. An ocean feature dominates the center of the image and appears to emanate from the south tip of the island. This feature lies to the north of a warm anti-cyclonic eddy and is capped by a cold cyclonic eddy outlined by a warm intrusion in the upper right portion. The upwelling south of the Island of Masirah is cold enough to saturate the white in the image. $2^{o}x2^{o}$ grid spacing. The southern tip of Masirah Island is at $20^{o}15'N$, $58^{o}40'E$, and the nearest grid intersection is $20^{o}N$, $58^{o}E$.

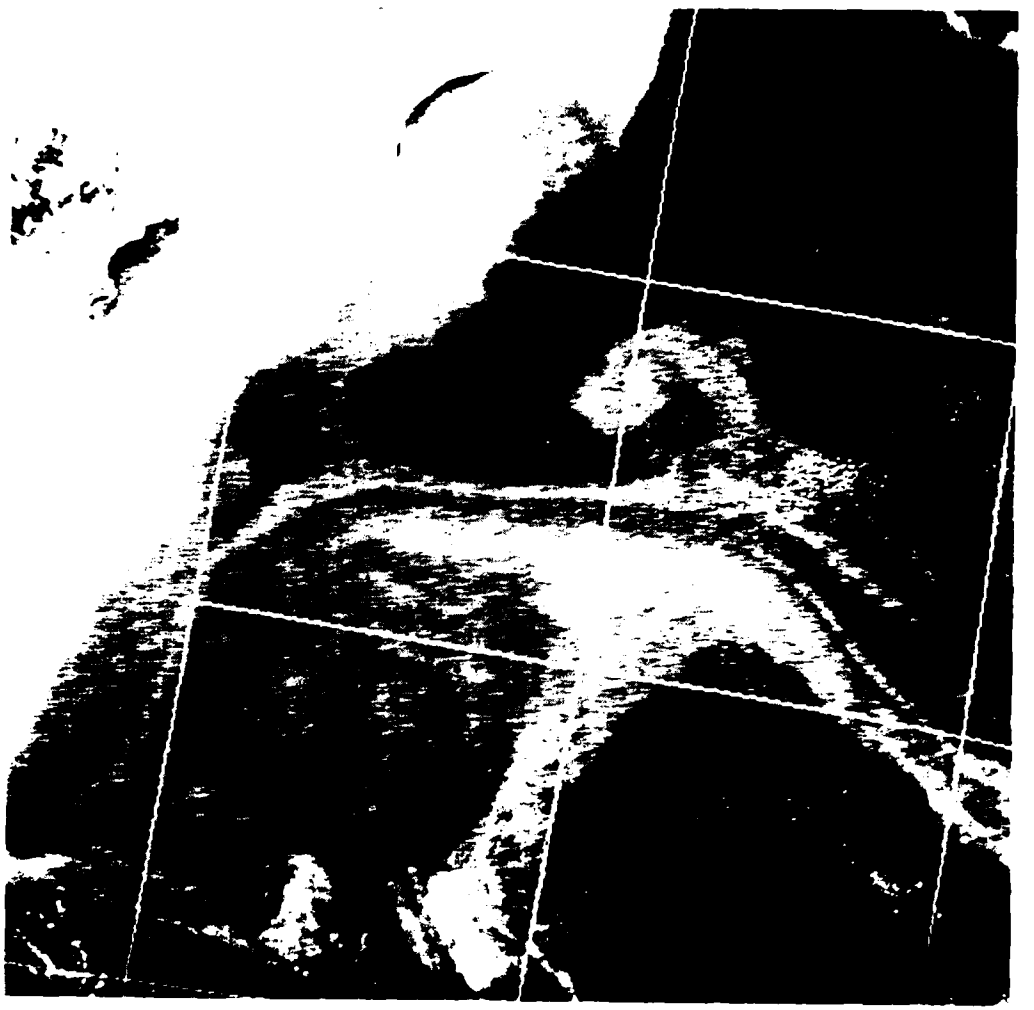

Figure 9. Coastal Region Off Arabian Peninsula.

The coastal region is shown from Ra's Madrakah to Ra's Mirbat. A large group of features dominates the field of view with cyclonic cold eddies and anticyclonic warm eddies outlined by cold features. Upwelling appears south of Ra's Madrakah. $2^{o}x2^{o}$ grid spacing. Ra's Madrakah in the top center is at $19^{o}0'N$, $57^{o}50'E$, with the nearest grid intersection at $18^{o}N$, $60^{o}E$.

Figure 10. Coastal Region Off Arabian Peninsula.

The coastal region is shown from Ra's Mirbat to Ra's Fartak. The Island of Socotra appears in the lower center of the image. Ocean thermal features are seen filling the entrance to the Gulf of Aden between Socotra Island and Ra's Fartak and beyond to Ra's Mirbat. $2^{o}x2^{o}$ grid spacing. The eastern tip of Socotra Island is at $12^{o}30'N$, $54^{o}30'E$. Ra's Mirbat is at $17^{o}15'N$, $55^{o}20'E$ and Ra's Fartak is at $15^{o}35'N$, $52^{o}15'E$.

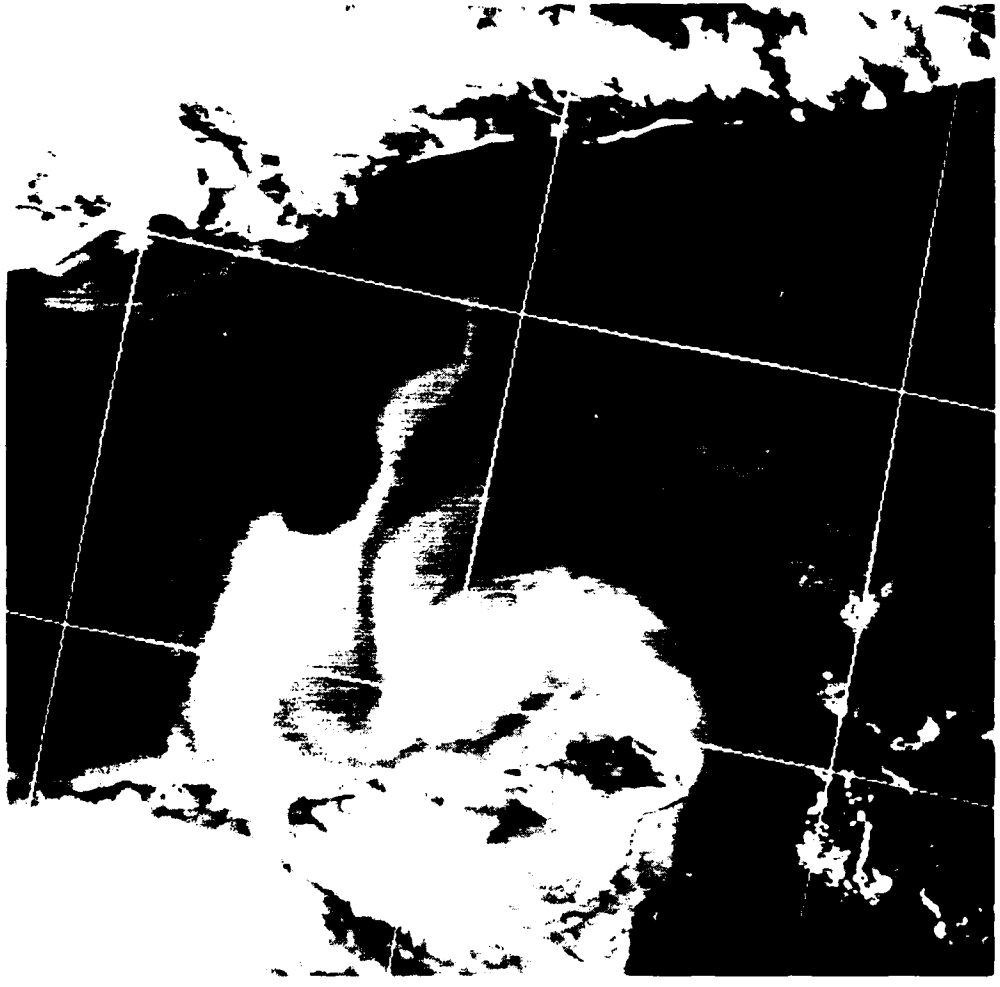

Figure 11. Gulf of Aden.

The entrance to the Gulf of Aden is shown between the Horn of Africa and the coast of the Arabian Peninsula. A faint tip of the western point of the Island of Socotra appears in the extreme right. Ocean thermal features dominate this region between the coast of the Arabian Peninsula, the Horn of Africa, and the Island of Socotra. $2^{o}x2^{o}$ grid spacing. The tip of the Horn of Africa (Ra's Aser) is at $11^{o}45'N$, $51^{o}20'E$.

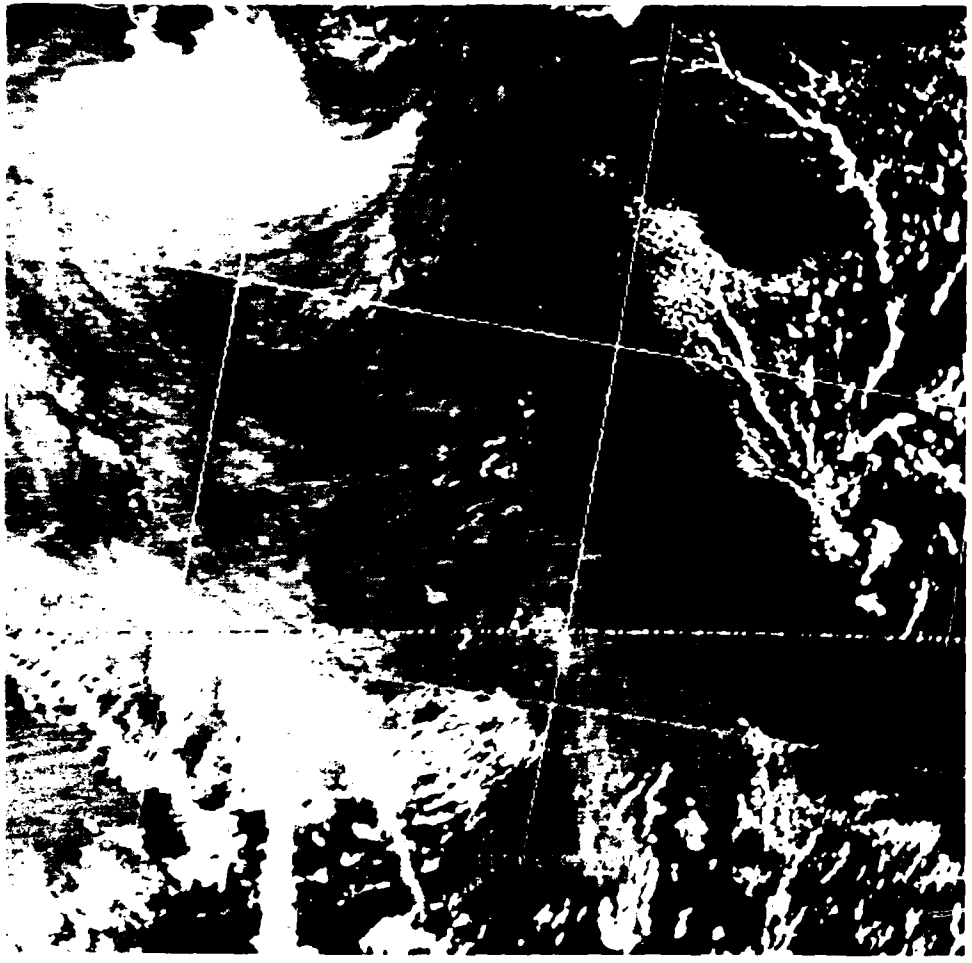

Figure 12. Ocean Region Near Horn of Africa.

The ocean region to the east and southeast of the Horn of Africa is shown. The Island of Socotra appears in the upper left. Clouds overlie portions of the view but weak thermal features to the southeast of Socotra Island suggest the demise of the Southwest Monsoon. $2^{o}x2^{o}$ grid spacing. The east tip of Socotra island is at $12^{o}30'N$, $54^{o}30'E$.

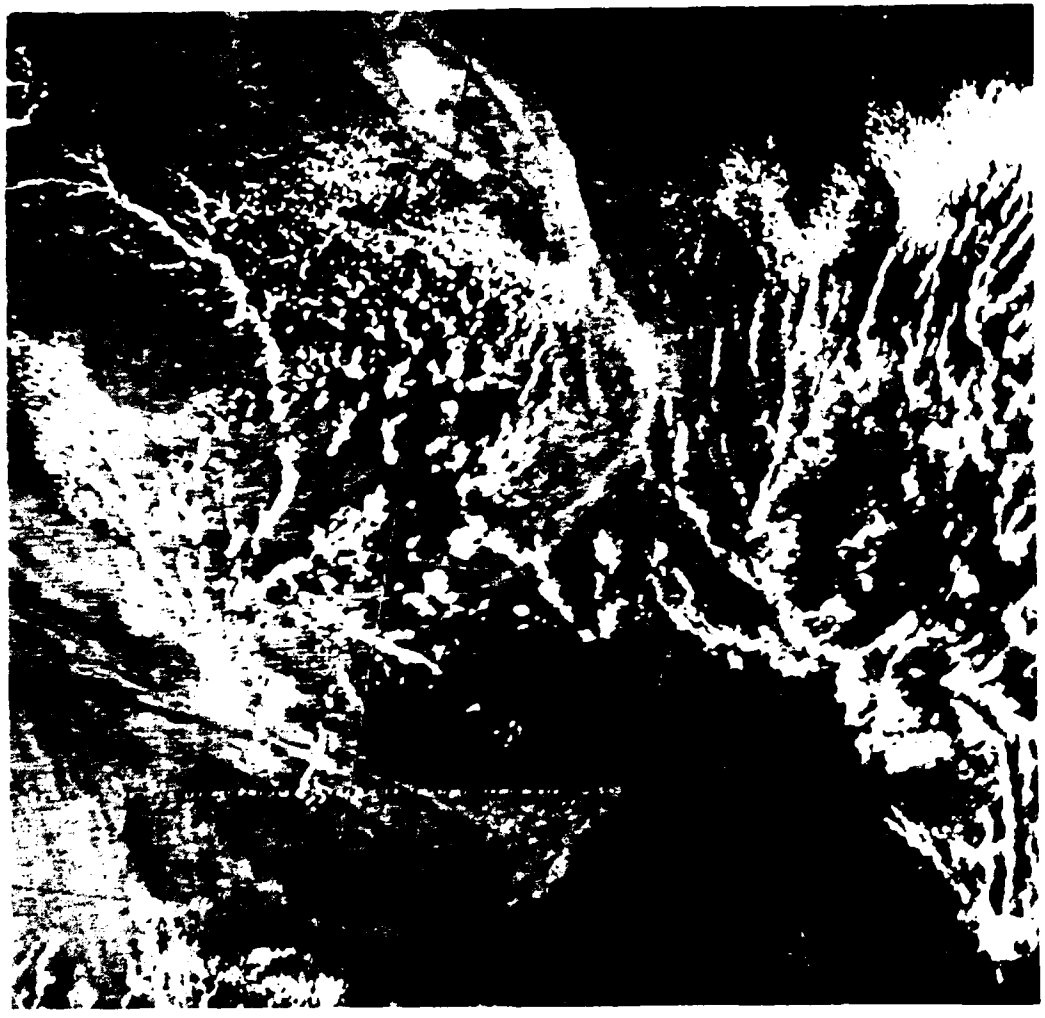

Figure 13. Ocean Region East of Socotra Island.

The next adjacent region of the ocean east of Figure 12 is shown. The cloud pattern in the left portion is the cloud pattern seen in the right portion of Figure 12. Some extension of ocean features seen in Figure 12 can be followed through the cloud patterns. $2^{o} \times 2^{o}$ grid apacing.

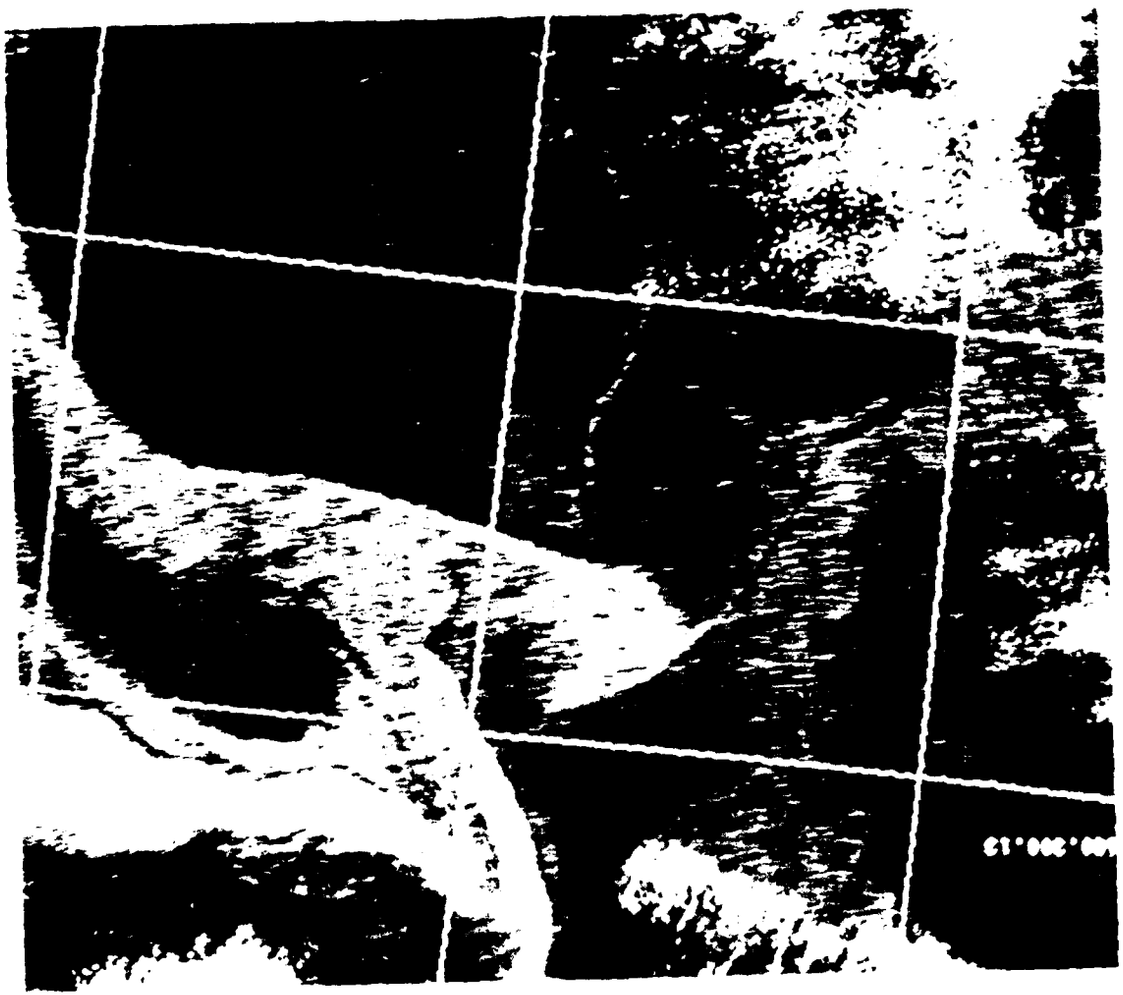

Figure 14. Western Portion of Upper Arabian Sea.

A region east of Ra's Fartak and south of Ra's al Hadd is shown. This view shows the continuation of the ocean thermal feature south of the feature in Figure 8 and east of the feature shown in Figure 9. $2^{o}x2^{o}$ grid spacing. The feature lies along $16^{o}N$, mostly between $60^{o}E$ and $62^{o}E$. It bifurcates east of $62^{o}E$.

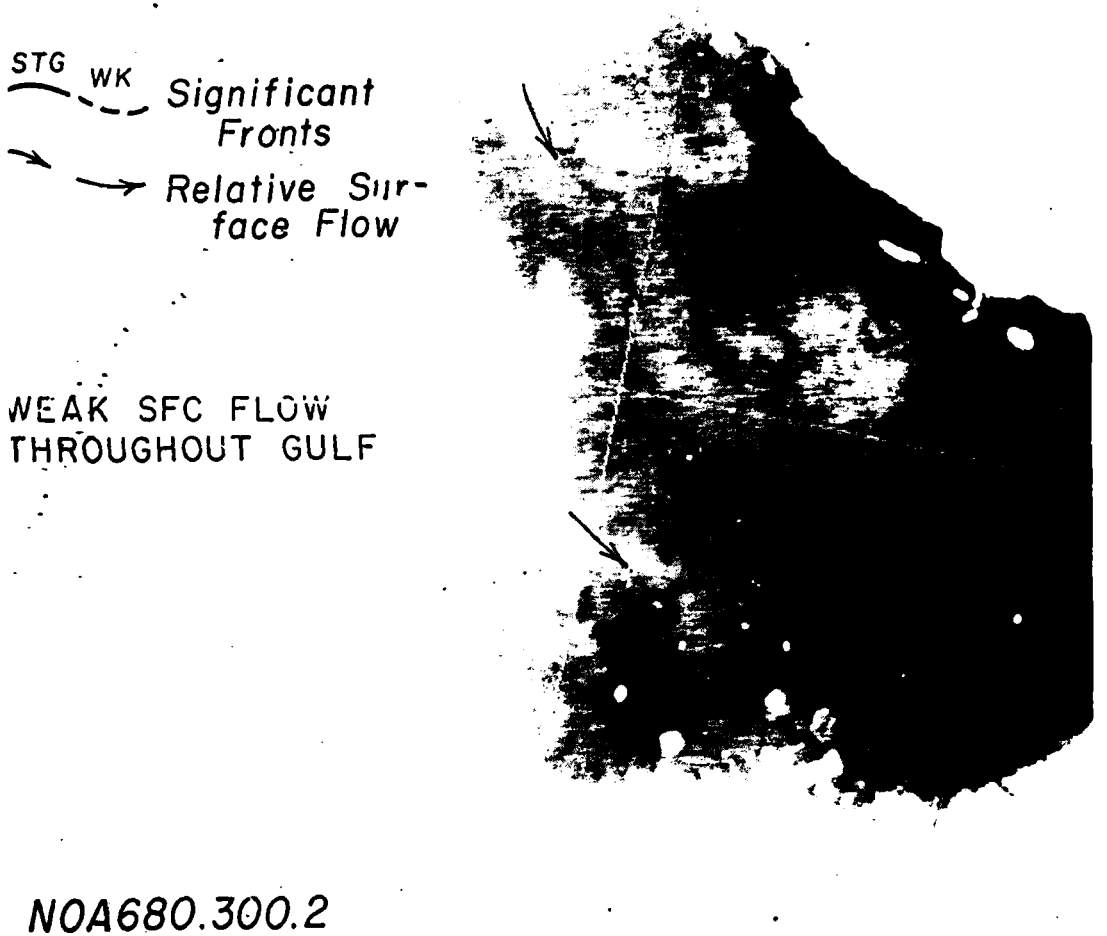

Figure 15. Persian Gulf.

The interpretation is shown for the ocean thermal feature which appears in Figure 4. A weak (wk) front is shown surrounding the feature. The legend indicates NOAA-6, 1980, Julian 300, enhanced image number two.

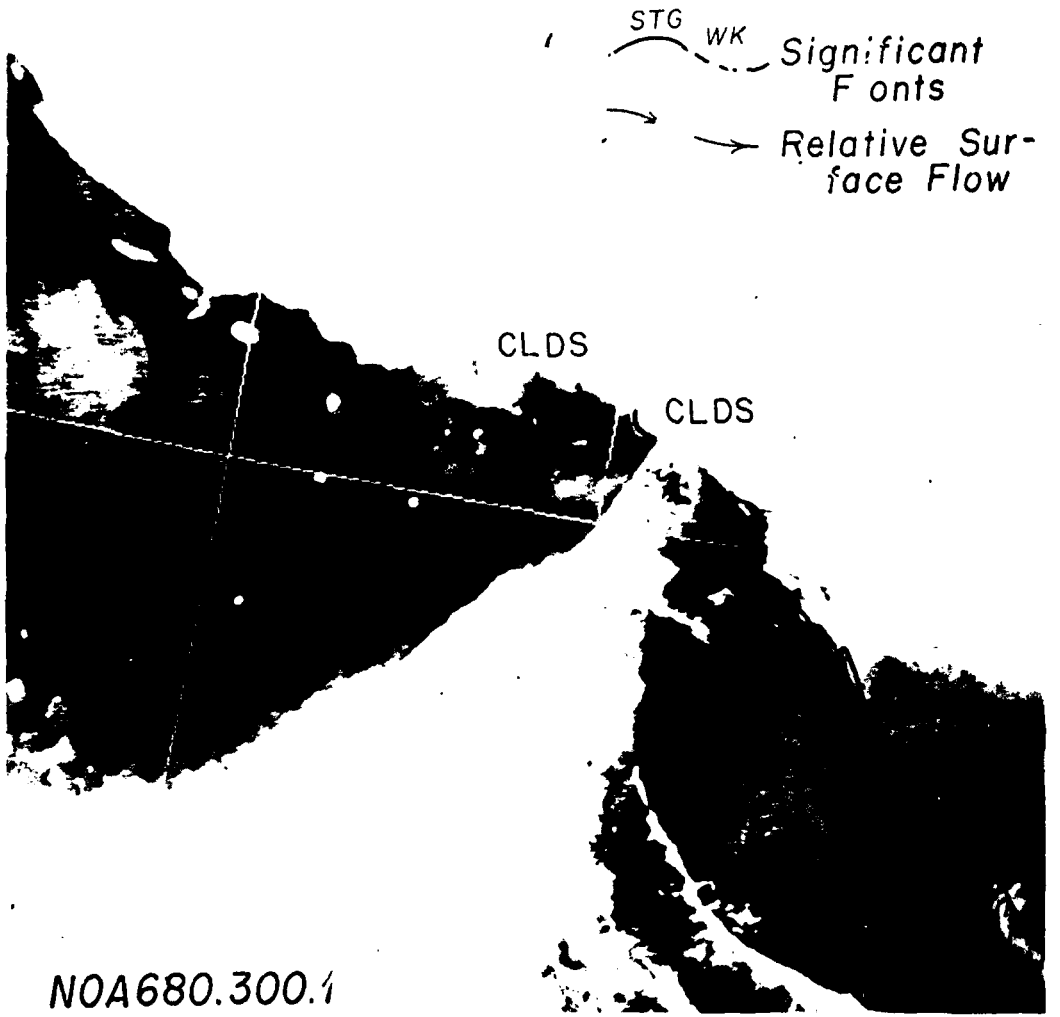

Figure 16. Strait of Hormuz.

The interpretation is shown for the image in Figure 5. Both strong (stg) and weak (wk) ocean fronts are indicated with clouds (clds) overlying the strait. The legend indicates NOAA-6, 1980, Julian 300, enhanced image number one.

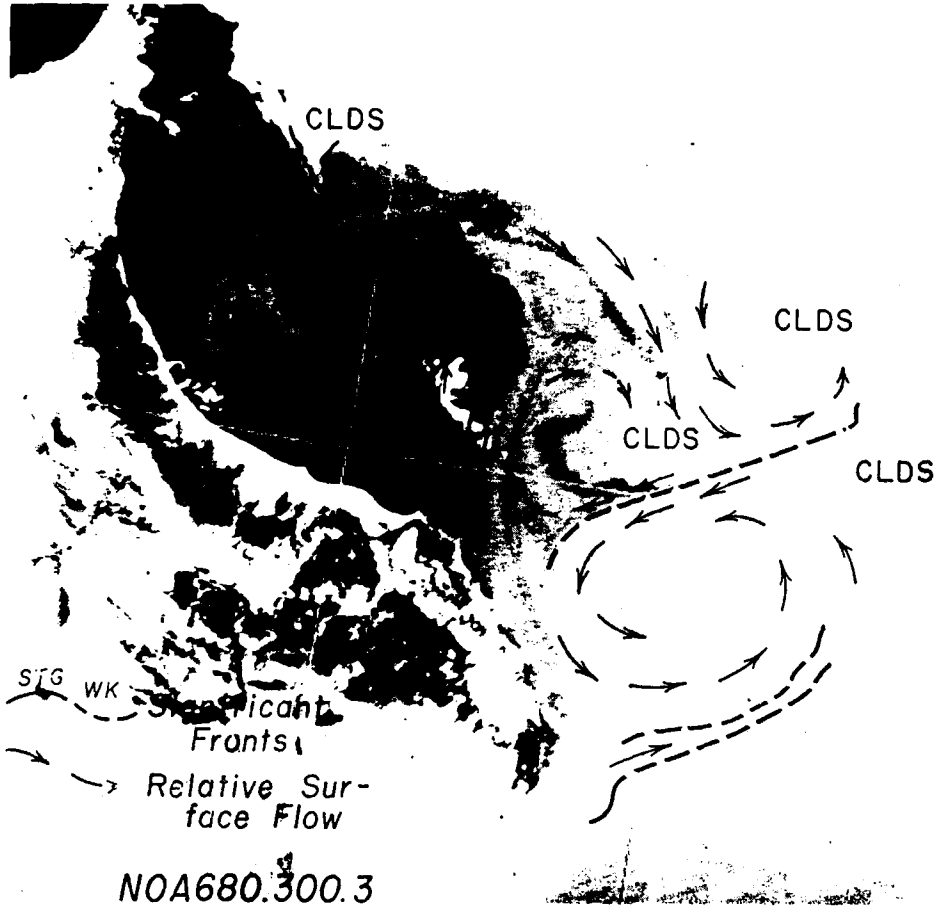

Figure 17. Gulf of Oman.

The interpretation is shown for the image in Figure 6. The shallow features in Figure 16 show in the upper left portion of this figure. Both strong (stg) and weak (wk) ocean fronts are indicated as well as ocean eddies. Clouds (clds) overlie much of the land and a portion of the right center image. A large cyclonic cold eddy is seen in the Gulf of Oman between Muscat and Ra's al Hadd which is affected near shore by light winds directed by the mountains between Muscat and Ra's al Hadd. The legend indicates NOAA-6, 1980, Julian 300, enhanced image number three.

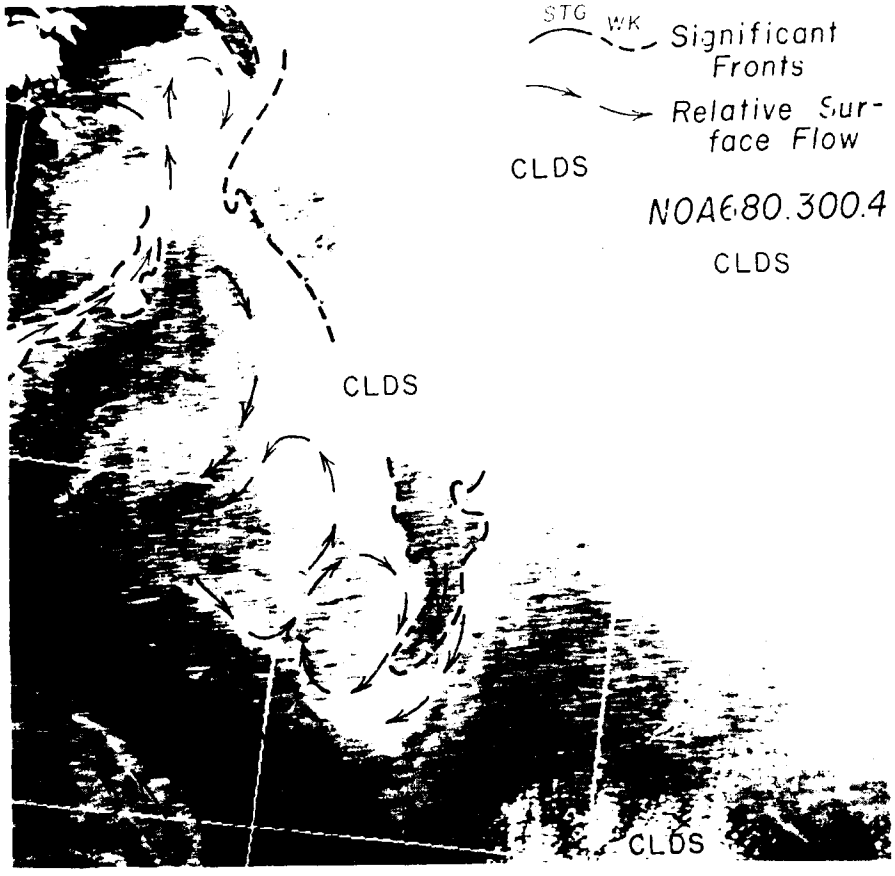

Figure 18. Gulf of Oman.

The interpretation is shown for the image in Figure 7. Several weak (wk) ocean fronts are indicated in the region not covered by clouds (clds). The edge of a cold cyclonic eddy appears in the left portion which also appears in the right portion of Figure 17. A warm intrusion is indicated in the lower left between a cold eddy in the extreme lower left and several eddies near the middle of the lower left. The legend indicates NOAA-6, 1980, Julian 300, enhanced image number four.

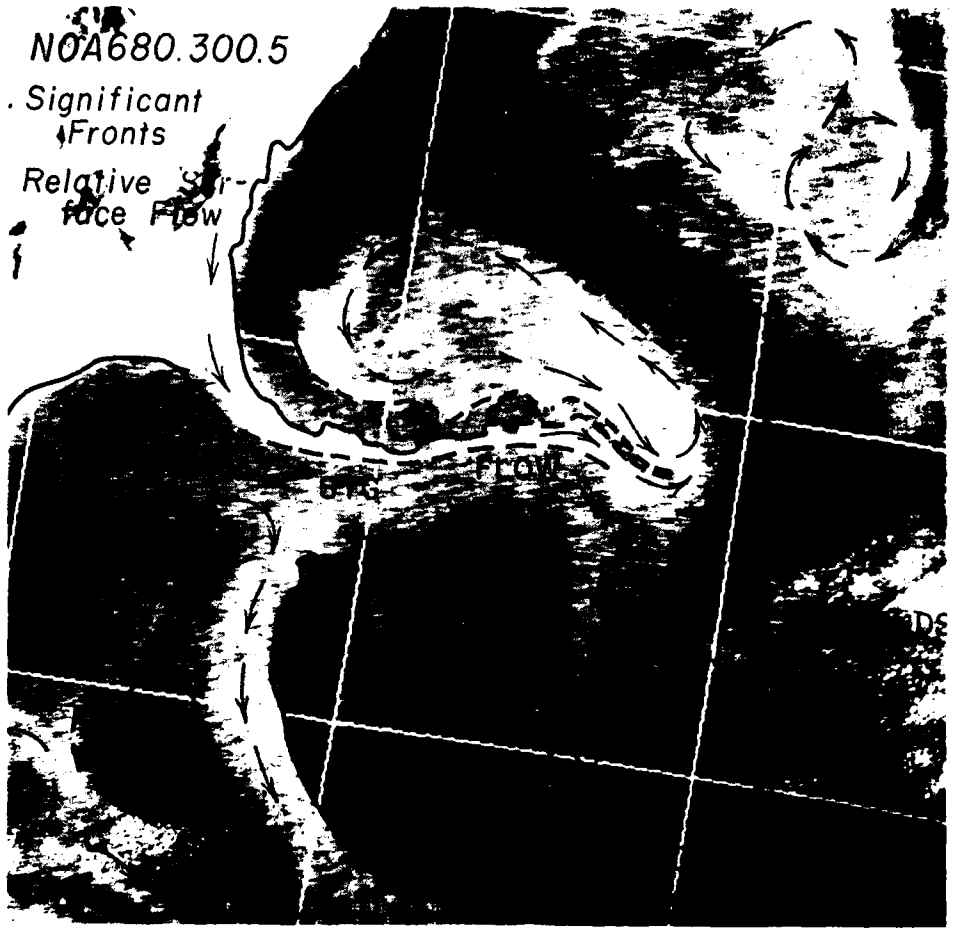

Figure 19. Coastal Region South of Gulf of Oman.

The interpretation is shown for the image in Figure 8. A strong (stg) flow is indicated associated with a major feature which propagates from upwelling off the south tip of the Island of Masirah. A cold cyclonic eddy is indicated to the north of this tongue-like feature. A sequence of warm and cold eddies is indicated in progression down the coast of the Arabian Peninsula, and major features associated with points of land are repeated along the coast. The legend indicates NOAA-6, 1980, Julian 300, enhanced image number five.

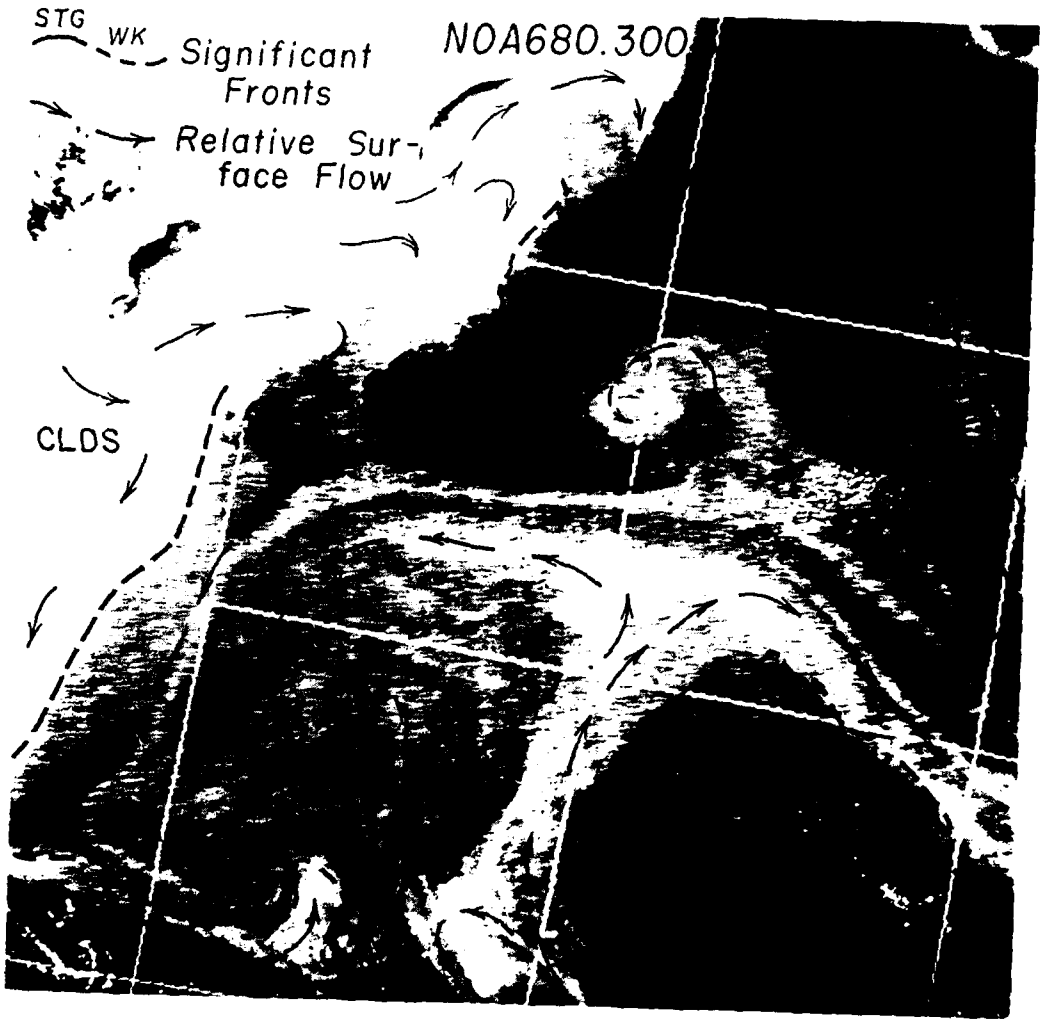

Figure 20. Coastal Region Off Arabian Peninsula.

The interpretation is shown for the image in Figure 9. Both strong (stg) and weak (wk) ocean fronts are indicated. There is a continuation of warm eddies surrounded by cold features in this progression down the coast of the Arabian Peninsula. A small cold cyclonic eddy is indicated near the center of the image. The legend indicates NOAA-6, 1980, Julian 300, enhanced image number six.

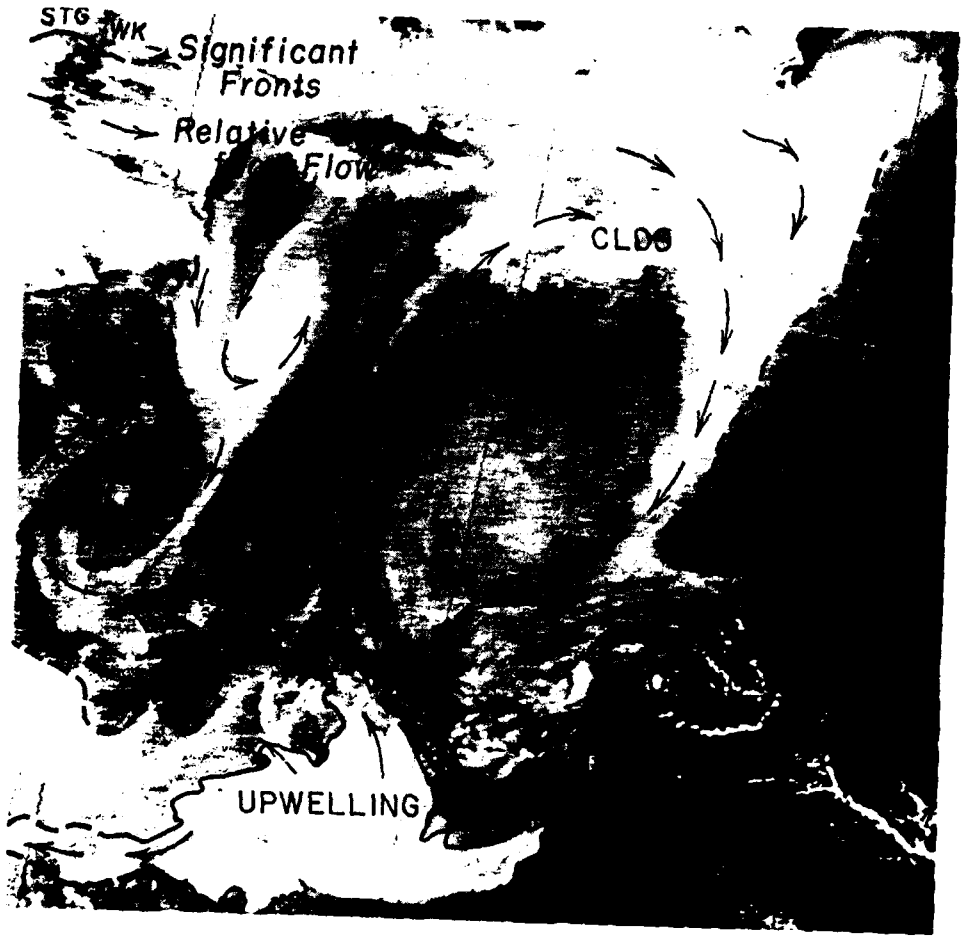

Figure 21. Coastal Region Off Arabian Peninsula.

The interpretation is shown for the image in Figure 10. Upwelling is apparent north and to the sides of the Island of Socotra. A large anticyclonic eddy is indicated in the eddy field north of the island. Several weak (wk) ocean fronts are indicated. This image shows the setup of the eddy field in the entrance to the Gulf of Aden between Socotra and the Arabian Peninsula. Slicking in the lower right portion of the image is an indication of surface daytime heating which has not been mixed in the absence of winds. The legend indicates NOAA-6, 1980, Julian 300, enhanced image number seven.

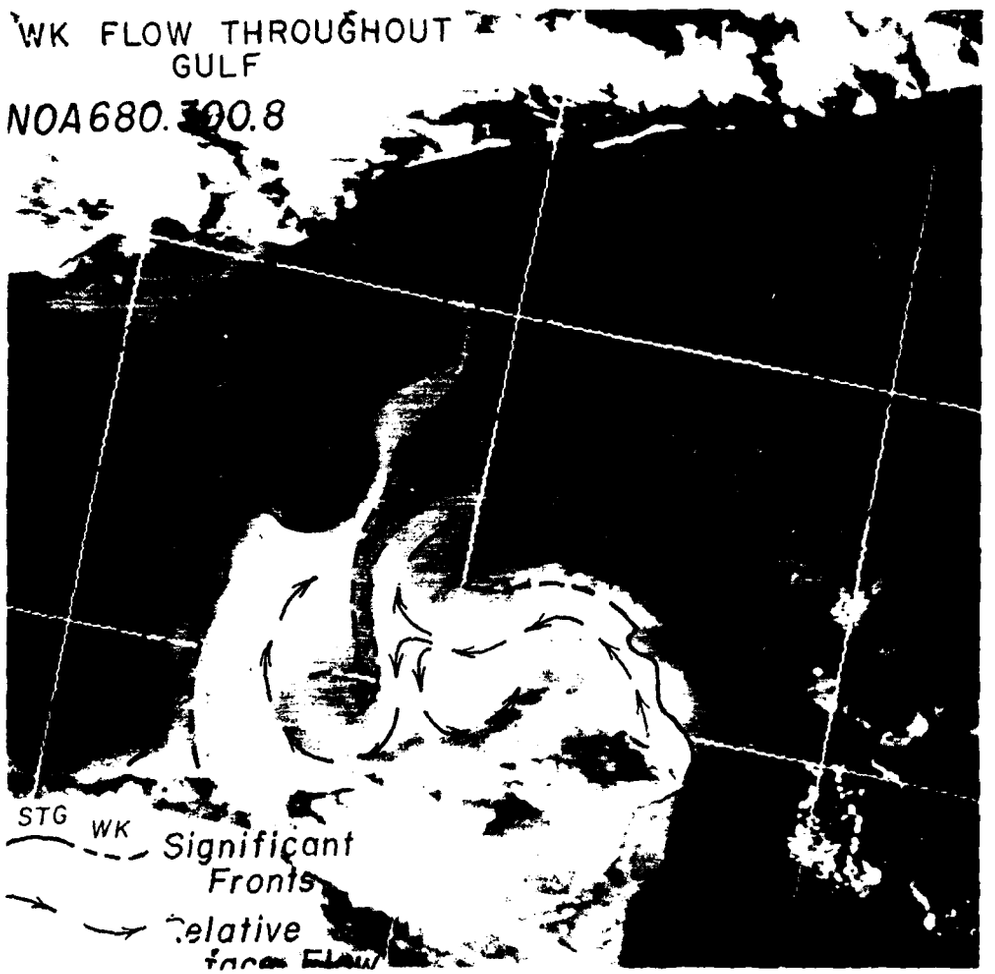

Figure 22. Gulf of Aden.

The interpretation is shown for the image in Figure 11. A continuation of the thermal structure and eddy field at the entrance to the Gulf of Aden is shown in this image progressing into the gulf. There is upwelling off the Horn of Africa and longshore flow near the coast of the Arabian Peninsula. Both strong (stg) and weak (wk) ocean fronts are indicated. The legend indicates NOAA-6, 1980, Julian 300, enhanced image number eight.

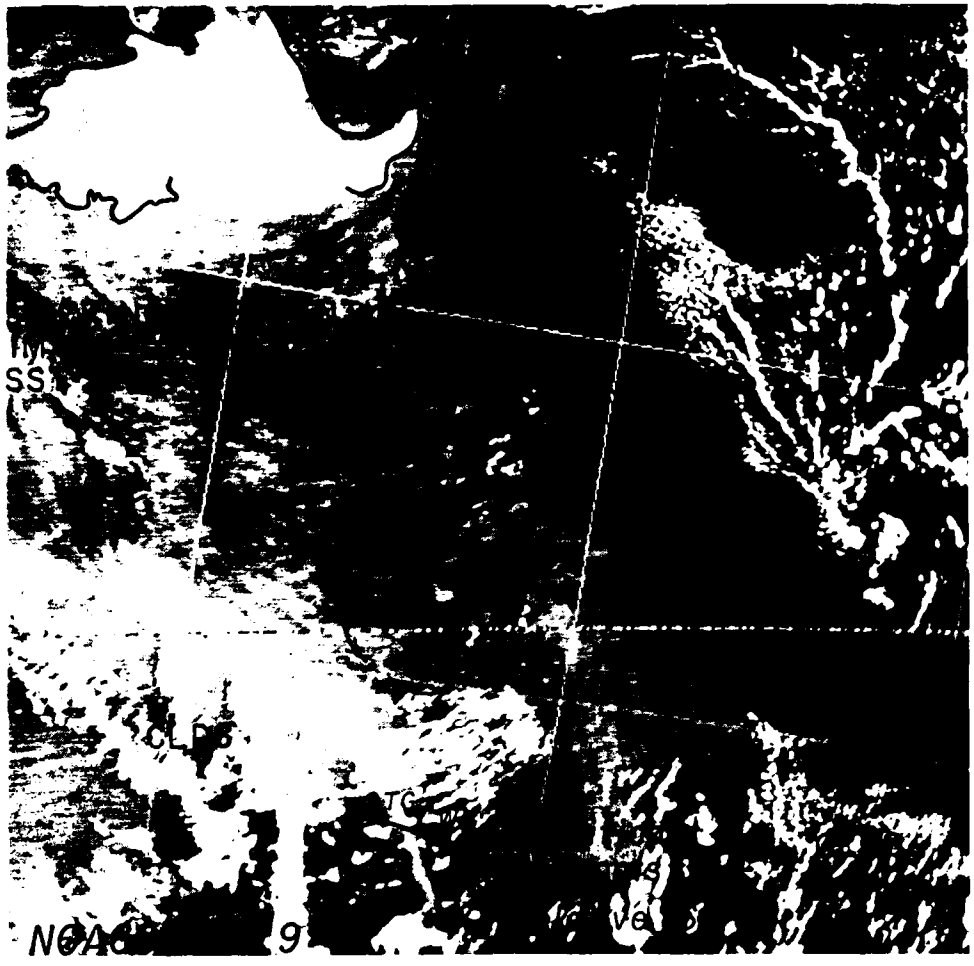

Figure 23. Ocean Region Near Horn of Africa.

The interpretation is shown for the image in Figure 12. The nature of the clouds (clds) is indicative of light winds in the area. In addition to the upwelling and strong (stg) frontal features associated with the Island of Socotra, the ocean thermal field is dominated by slicking patterns. The slicking, caused by daytime heating, has remained on the surface due to the absence of winds. These slicking patterns tend to outline the relative surface flow. The legend indicates NOAA-6, 1980, Julian 300, enhanced image number nine.

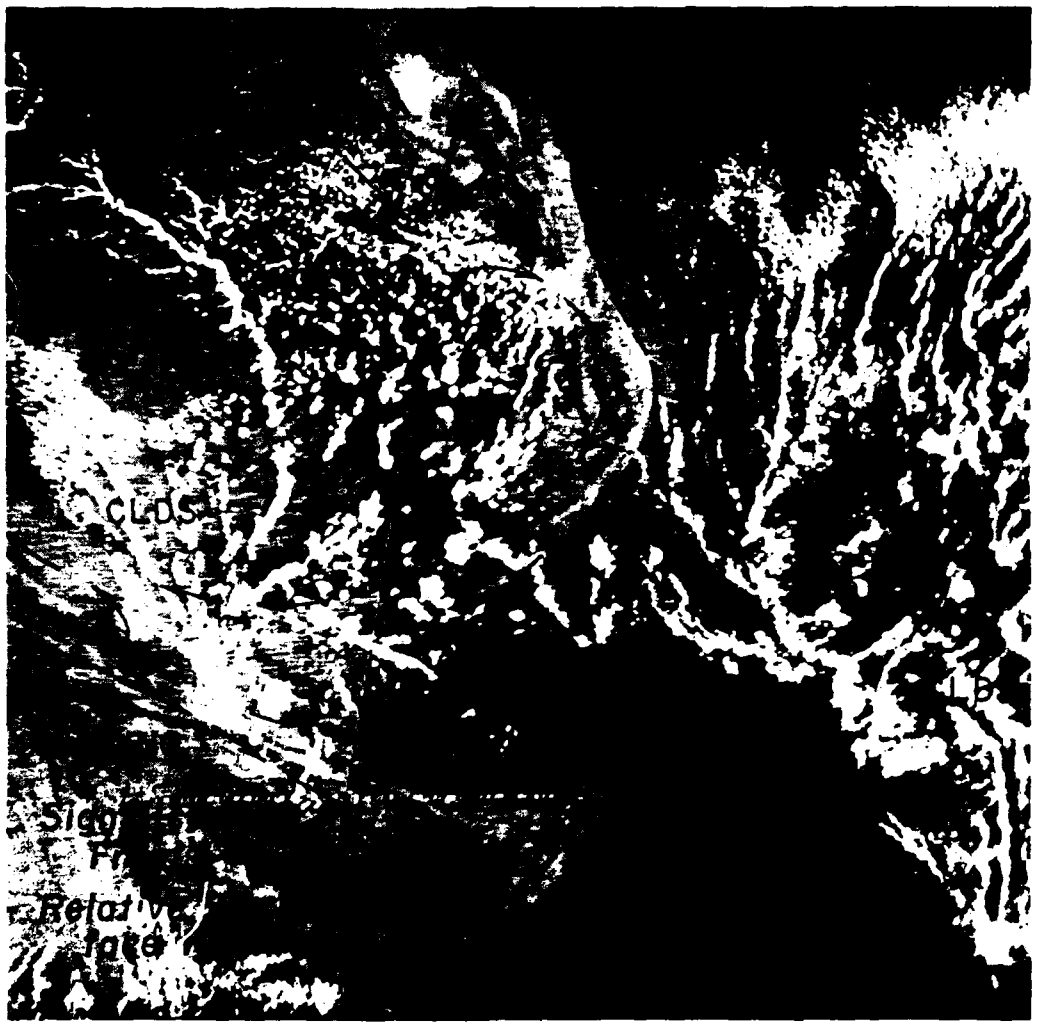

Figure 24. Ocean Region East of Socotra Island.

The interpretation is shown for the image in Figure 13. A continuation of the clouds (clds) and interpretive features in Figure 23 can be seen in this image which lies to the east of the area in Figure 23. The legend indicates NOAA-6, 1980, Julian 300, enhanced image number ten.

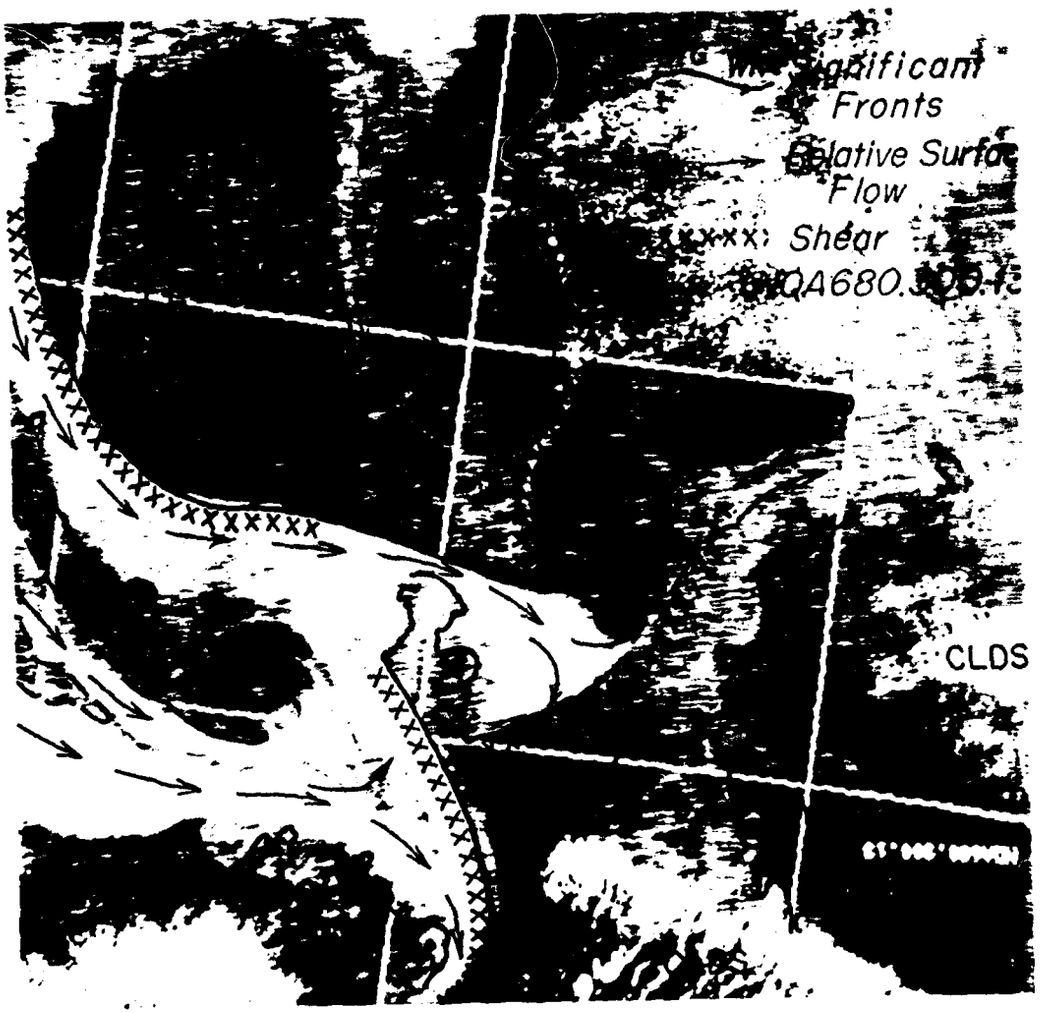

Figure 25. Western Portion of Upper Arabian Sea.

The interpretation is shown for the image in Figure 14. Substantial thermal structure is indicated in this image. This structure is the extension of structures closer to the Arabian Coast identified in Figures 19 and 20. The legend indicates NOAA-6, 1980, Julian 300, enhanced image number thirteen.

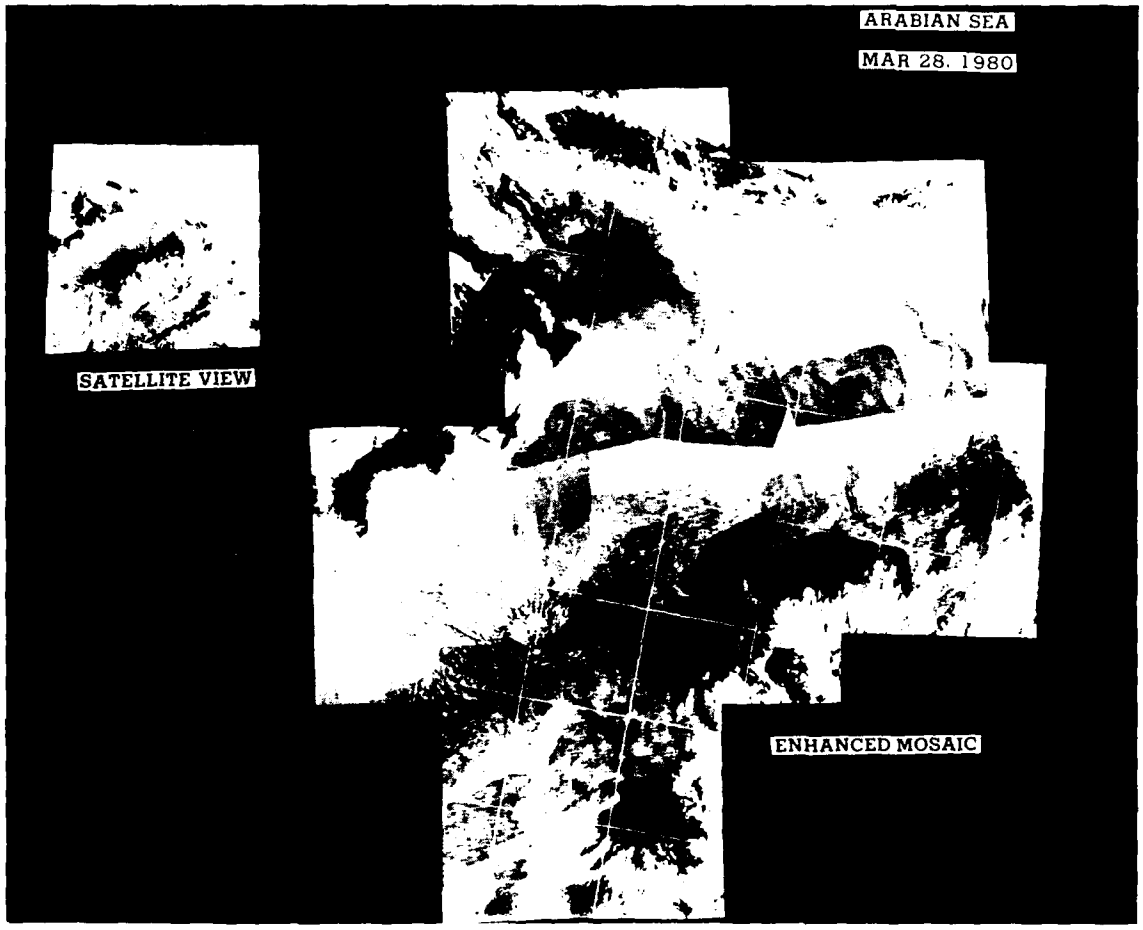

Figure 26. Arabian Sea Infrared Image Mosaic 28 March 1980.

A composite of enhanced images is shown with the Gulf of Oman and the coasts of Iran and Pakistan at the top, and the Arabian Peninsula coast on the left. Clouds appear in the lower right. Ocean thermal features dominate all of the view of the ocean surface. A separate low resolution satellite view from Channel Three of the NOAA-6 satellite appears left of the mosaic and indicates the data from which the composite was made.

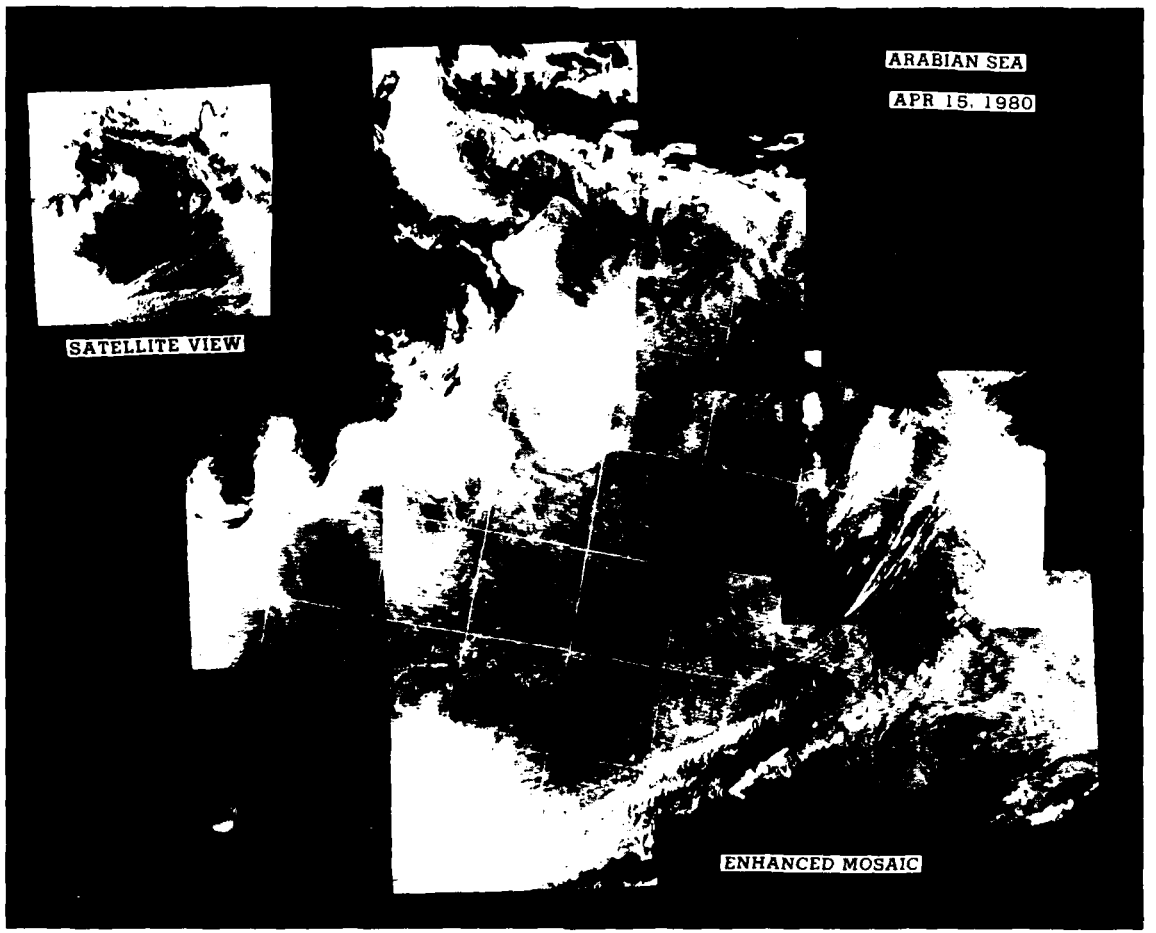

Figure 27. Arabian Sea Infrared Image Mosaic, 15 April 1980.

A composite of enhanced images is shown with the Gulf of Oman and coast of Iran at the top, and the Arabian Peninsula coast on the left. There are clouds in the lower right. Ocean thermal features appear over most of the view of the ocean surface. A separate low resolution satellite view from Channel Three of NOAA-6 appears left of the mosaic and indicates the data from which the composite was made.

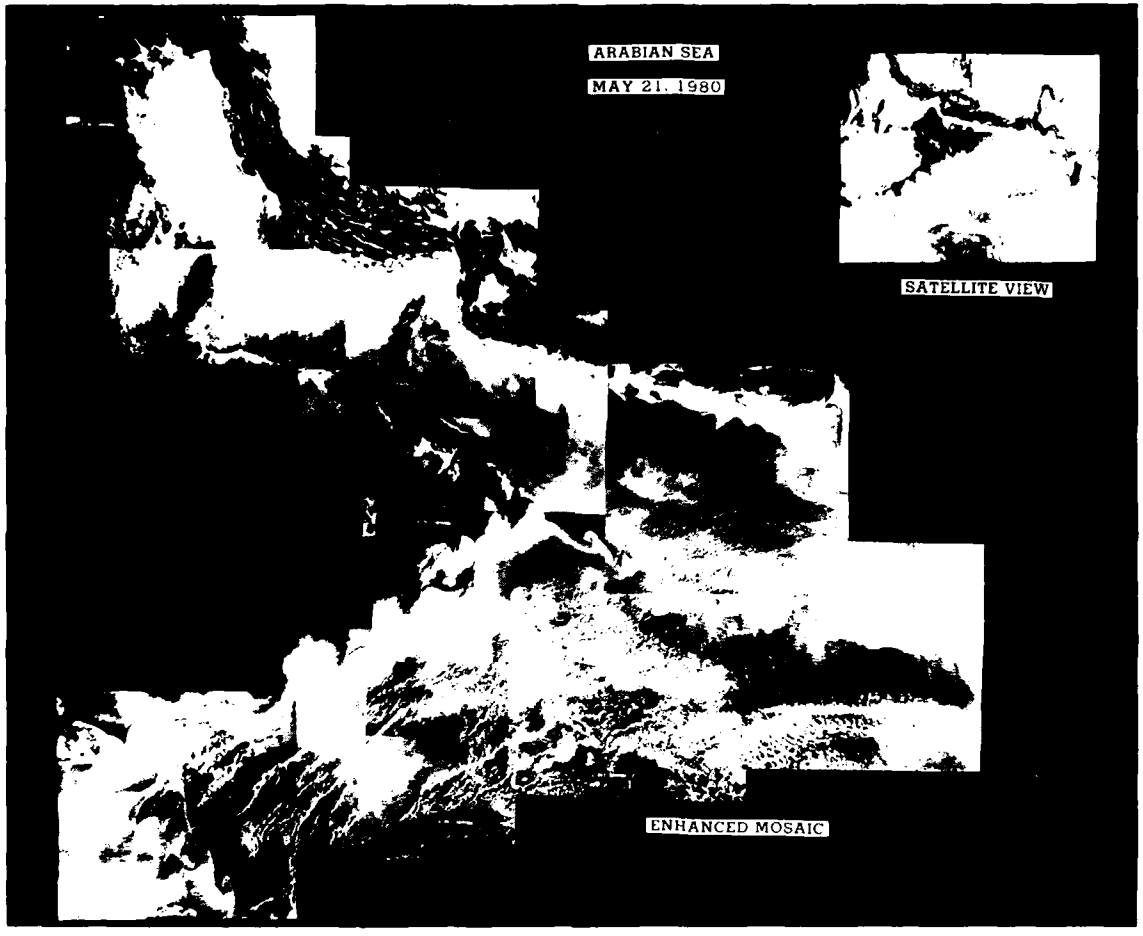

Figure 28. Arabian Sea Infrared Image Mosaic, 21 May 1980.

A composite of enhanced images is shown with the Persian Gulf, Strait of Hormuz, Gulf of Oman, and coast of Iran at the top, and the Arabian Peninsula coast on the left. Cloud bands dominate the ocean view and illustrate the beginning of the summer Southwest Monsoon. Ocean thermal features can be seen where the ocean surface is exposed. A separate low resolution satellite view from Channel Three of NOAA-6 appears right of the mosaic and indicates the data from which the composite was made.

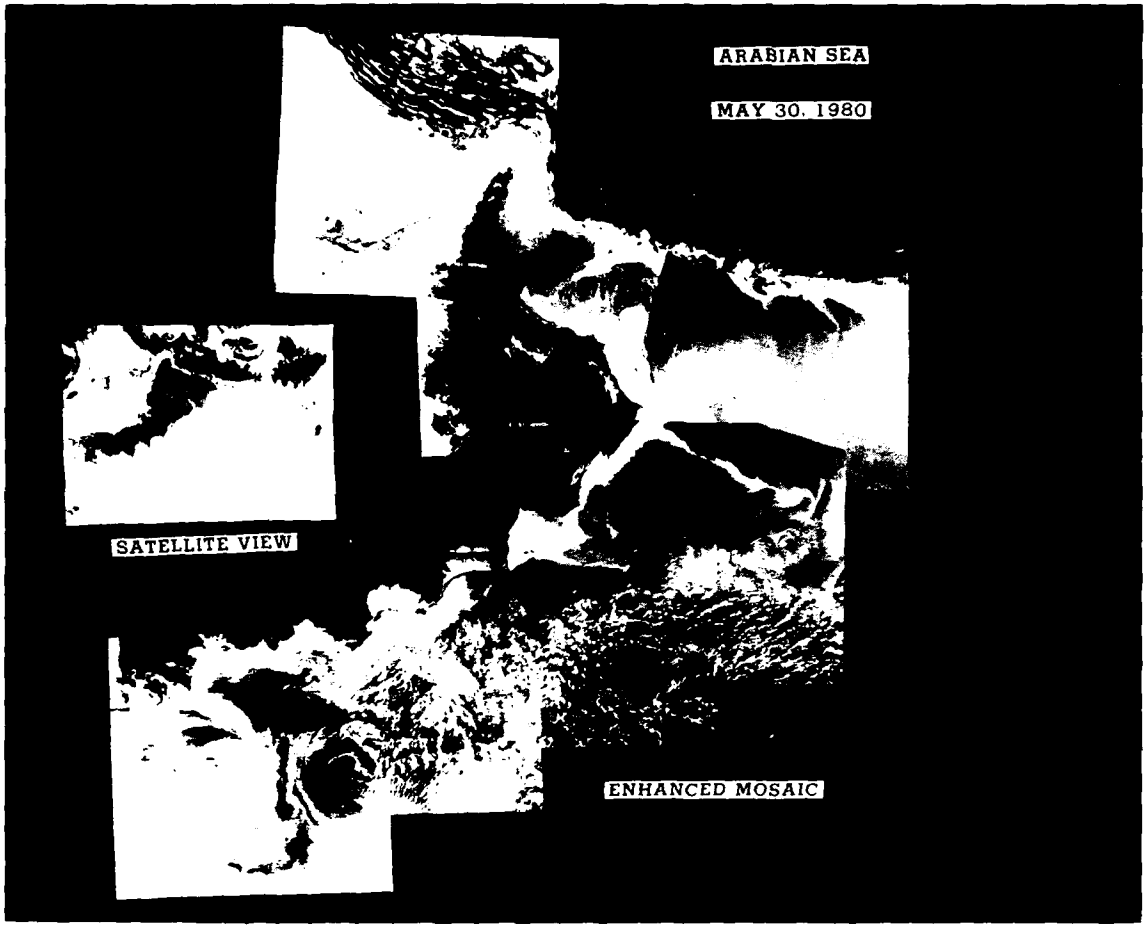

Figure 29. Arabian Sea Infrared Image Mosaic, 30 May 1980.

A composite of enhanced images is shown with the lower Persian Gulf, Strait of Hormuz, Gulf of Oman, and coast of Iran at the top, and the Arabian Peninsula coast on the left. The entrance to the Gulf of Aden can be seen as well as portions of the Island of Socotra. Clouds appear to dominate much of the ocean view. Strong ocean thermal features can be seen wherever the ocean surface is exposed, such as along the coast and in the Gulf of Oman. A separate low resolution satellite view from Channel Three of NOAA-6 appears left of the mosaic and indicates the data from which the composite was made.

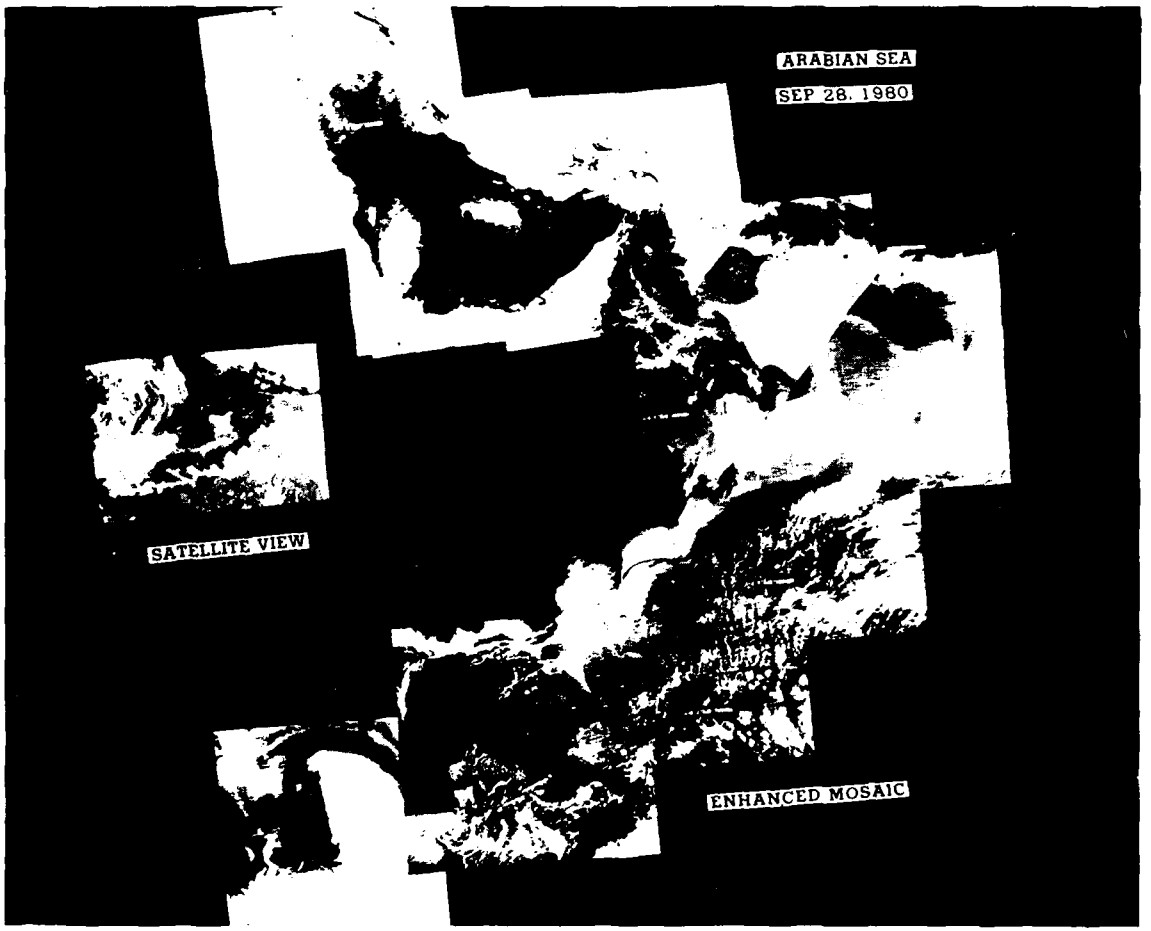

Figure 30. Arabian Sea Infrared Image Mosaic, 28 September 1980.

A composite of enhanced images is shown with the Persian Gulf, Strait of Hormuz, Gulf of Oman, and coast of Iran at the top, and the Arabian Peninsula coast on the left. Clouds cover most of the Arabian Sea but ocean thermal features can be seen where the ocean surface is exposed. A separate low resolution satellite view from Channel Three of NOAA-6 appears left of the mosaic and indicates the data from which the composite was made.

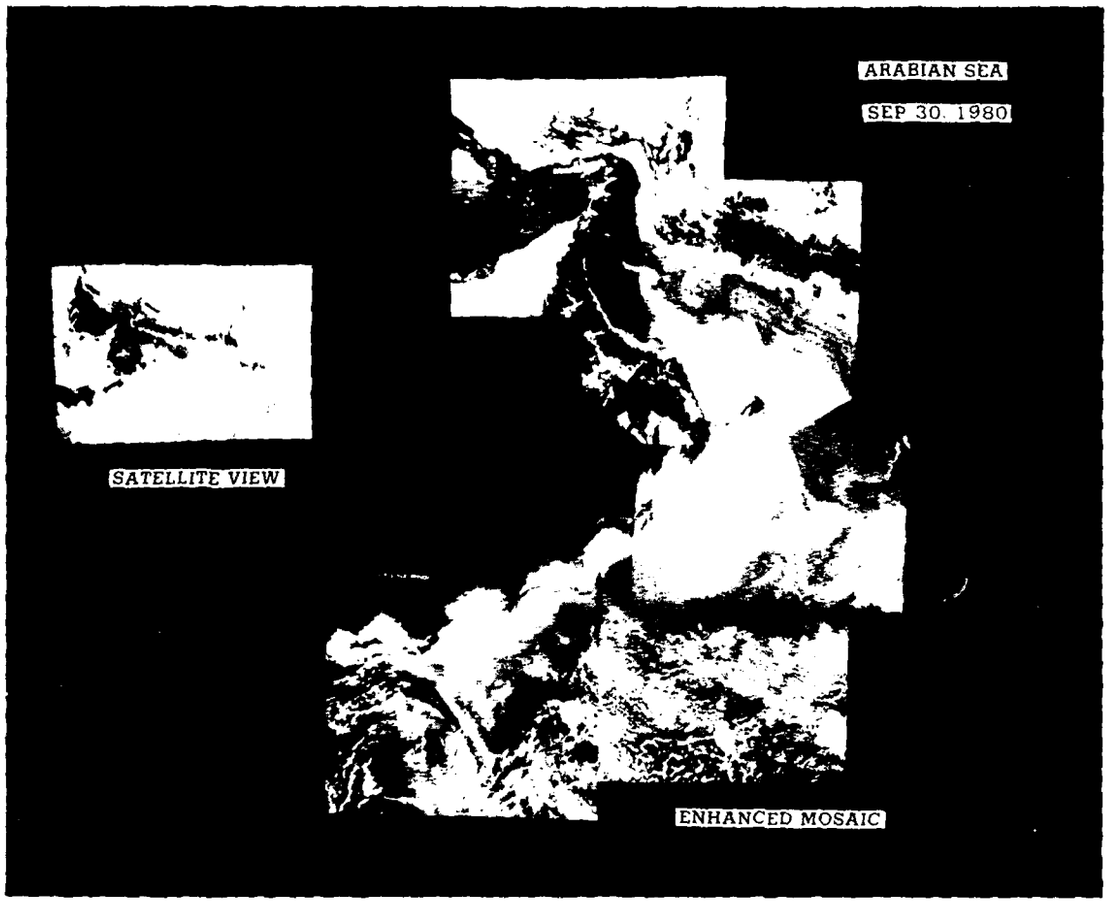

Figure 31. Arabian Sea Infrared Image Mosaic, 30 September 1980.

A composite of enhanced images is shown with the lower Persian Gulf, Strait of Hormuz, Gulf of Oman, and coast of Iran at the top, and the Arabian Peninsula coast on the left. Clouds appear on the lower portion. Strong ocean thermal features can be seen where the ocean surface is exposed. A separate low resolution satellite view from Channel Three of NOAA-6 appears left of the mosaic and indicates the data from which the composite was made.

Figure 32. Arabian Sea Infrared Image Mosaic, 26 October 1980.

A composite of enhanced images is shown with the lower Persian Gulf and Gulf of Oman at the top, and the Arabian Peninsula coast on the left. Clouds appear in the upper right and lower portions of the mosaic. Strong ocean thermal features can be seen wherever the ocean surface is exposed. A separate low resolution satellite view from Channel Three of NOAA-6 appears left of the mosaic and indicates the data from which the composite was made.

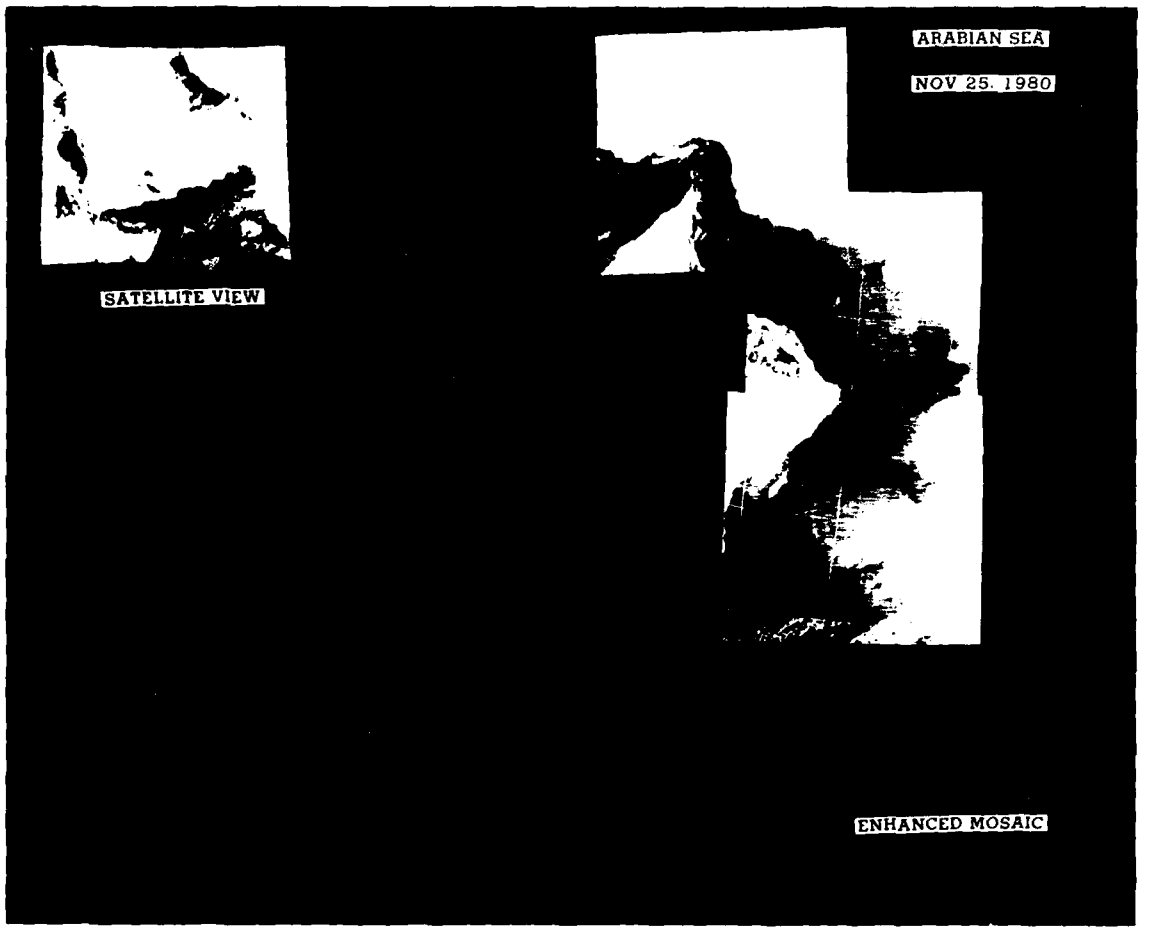

Figure 33. Arabian Sea Infrared Image Mosaic, 25 November 1980.

A limited composite of enhanced images is shown with the Strait of Hormuz, coast of Iran, and Gulf of Oman at the top, and a portion of the Arabian Peninsula coast in the left center. The Island of Masirah appears in the lower portion. Clouds appear on the right and weak ocean thermal features can be seen between the clouds and the Arabian Peninsula. A separate low resolution satellite view from Channel Three of NOAA-6 appears left of the mosaic and indicates the data from which the composite was made. The composite was limited due to masking by atmospheric moisture and absence of apparent ocean thermal structure in regions farther down the Arabian Coast.

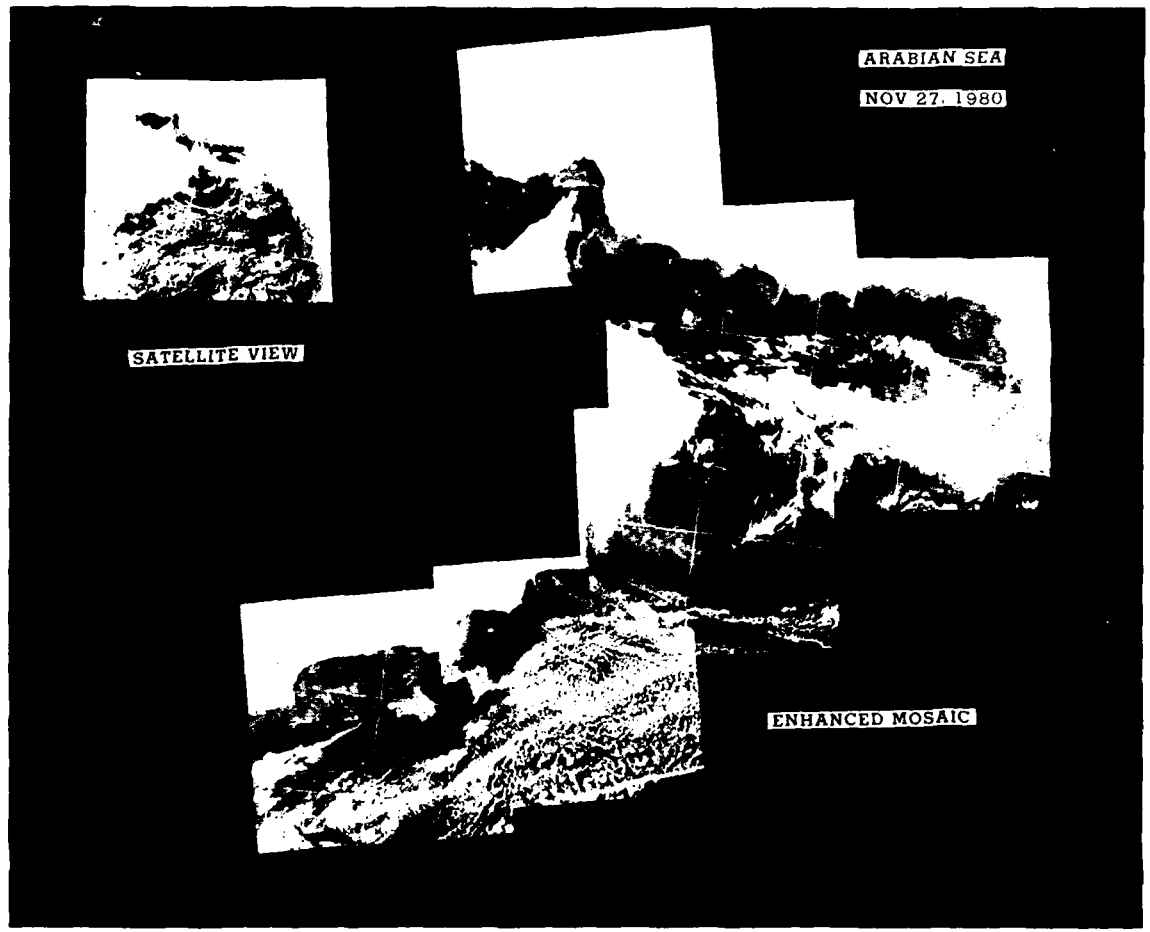

Figure 34. Arabian Sea Infrared Image Mosaic, 27 November 1980.

A composite of enhanced images is shown with the Strait of Hormuz, coast of Iran, and Gulf of Oman at the top, and the Arabian Peninsula coast on the left. Clouds dominate much of the field of view and weak ocean thermal features can be seen near the coast, becoming stronger in the Gulf of Aden. A separate low resolution satellite view from Channel Three of NOAA-6 appears left of the mosaic and indicates the data from which the composite was made.

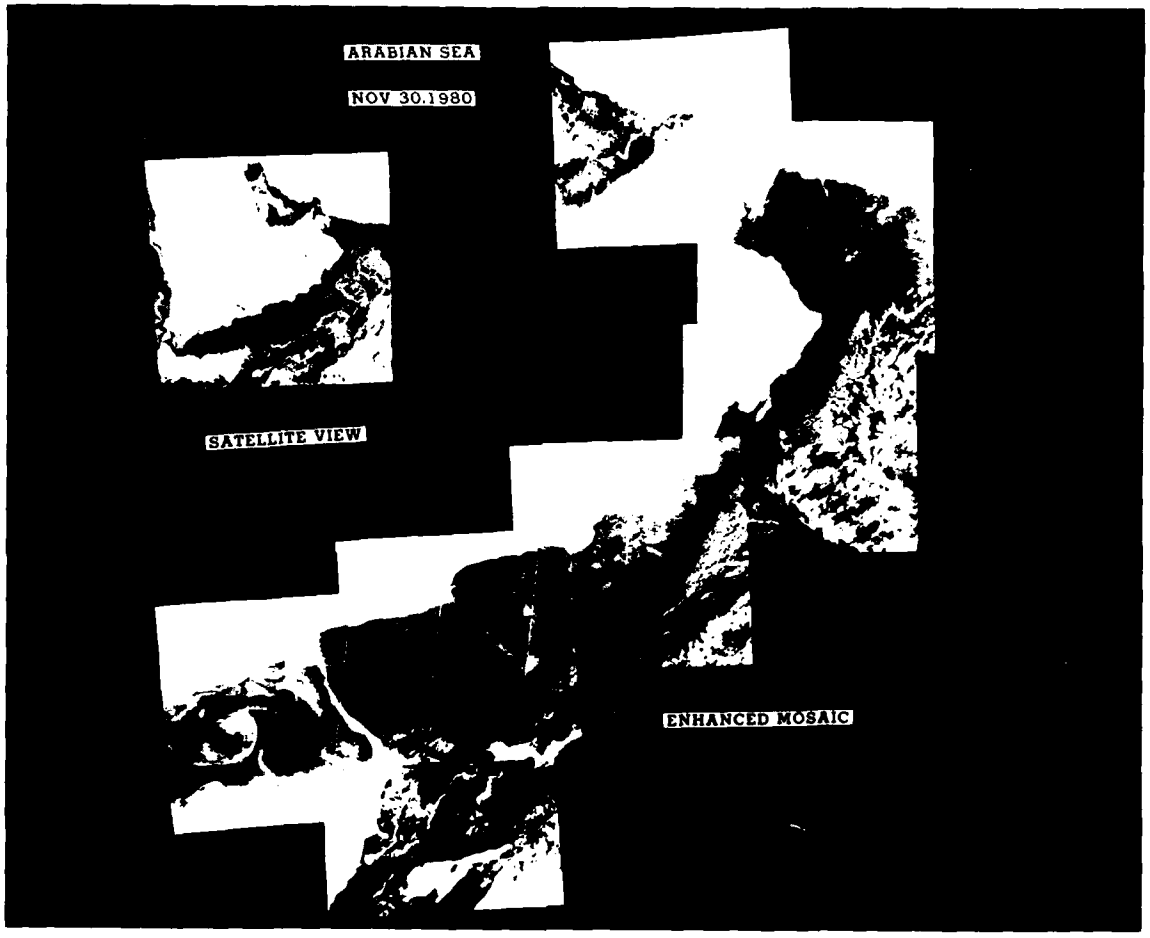

Figure 35. Arabian Sea Infrared Image Mosaic, 30 November 1980.

A composite of enhanced images is shown with the Strait of Hormuz and Gulf of Oman at the top and the Arabian Peninsula on the left. Clouds cover most of the Arabian Sea but some ocean thermal features can be seen where the ocean is exposed along the Arabian coast. A separate low resolution satellite view from Channel Three of NOAA-6 appears left of the mosaic and indicates the data from which the composite was made.

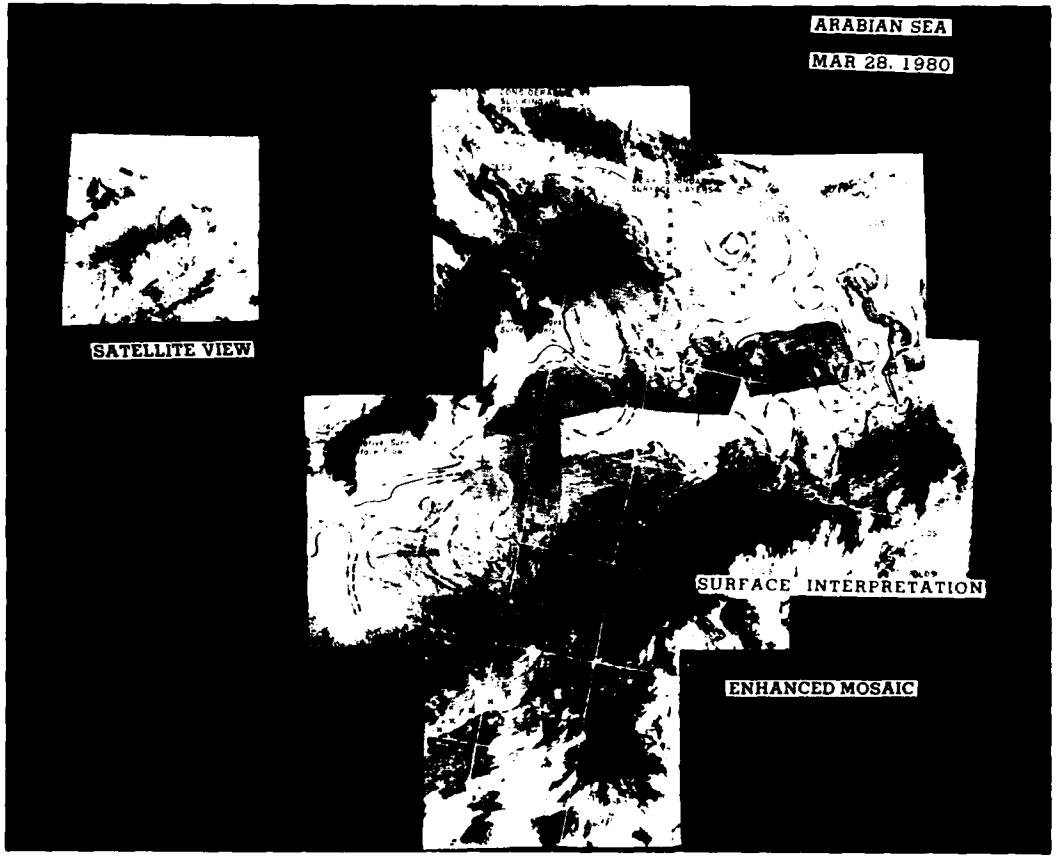

Figure 36. Arabian Sea Mosaic with Interpretation, 28 March 1980.

The composite of enhanced images shown in Figure 26 is shown here with a composite of surface interpretations for each image. Relative flow is indicated by arrows, and strong and weak fronts are indicated by solid and dashed lines respectively. Shear flow is indicated by a row of "x's". Slicking from daytime heating appears where there has been little surface mixing.

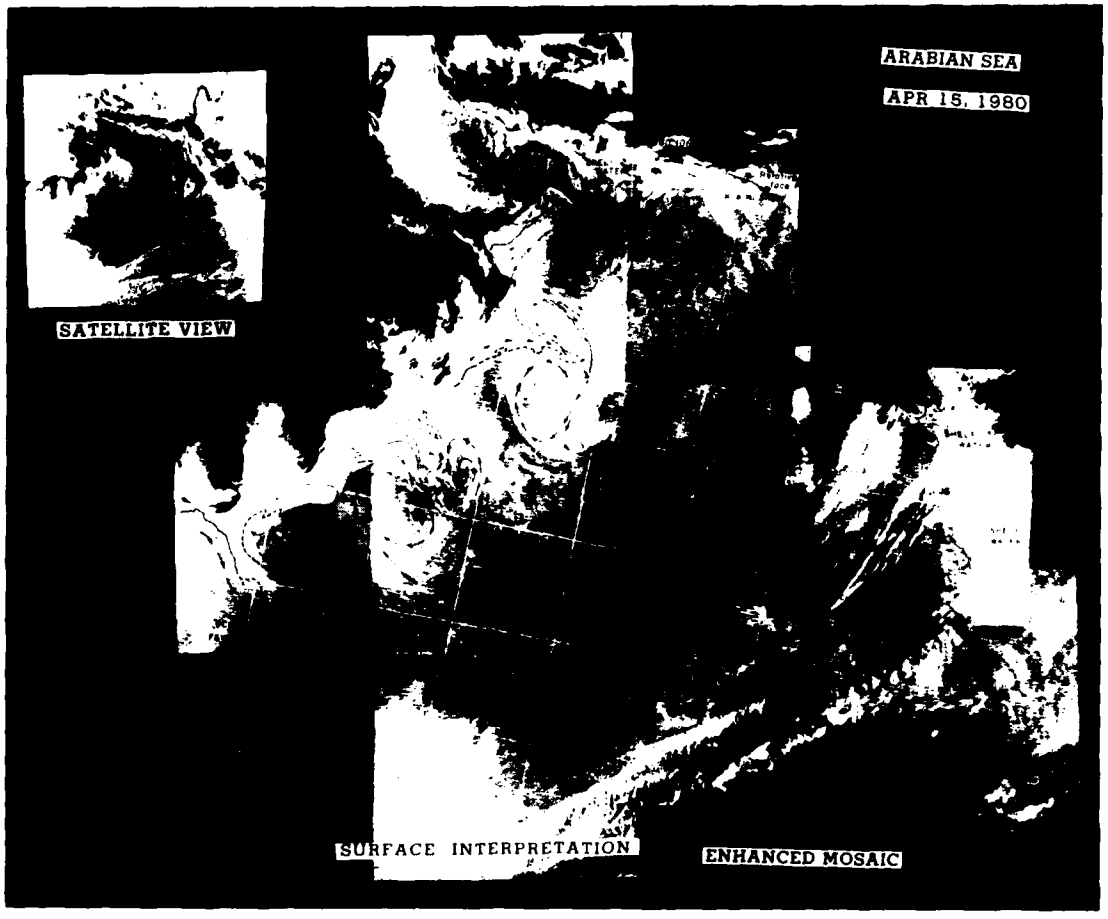

Figure 37. Arabian Sea Mosaic with Interpretation, 15 April 1980.

The composite of enhanced images shown in Figure 27 is shown here with a composite of surface interpretations for each image. Relative flow is indicated by arrows, and strong and weak fronts are indicated by solid and dashed lines respectively. (A poor alignment of lines indicating fronts occurred in the printing process.)

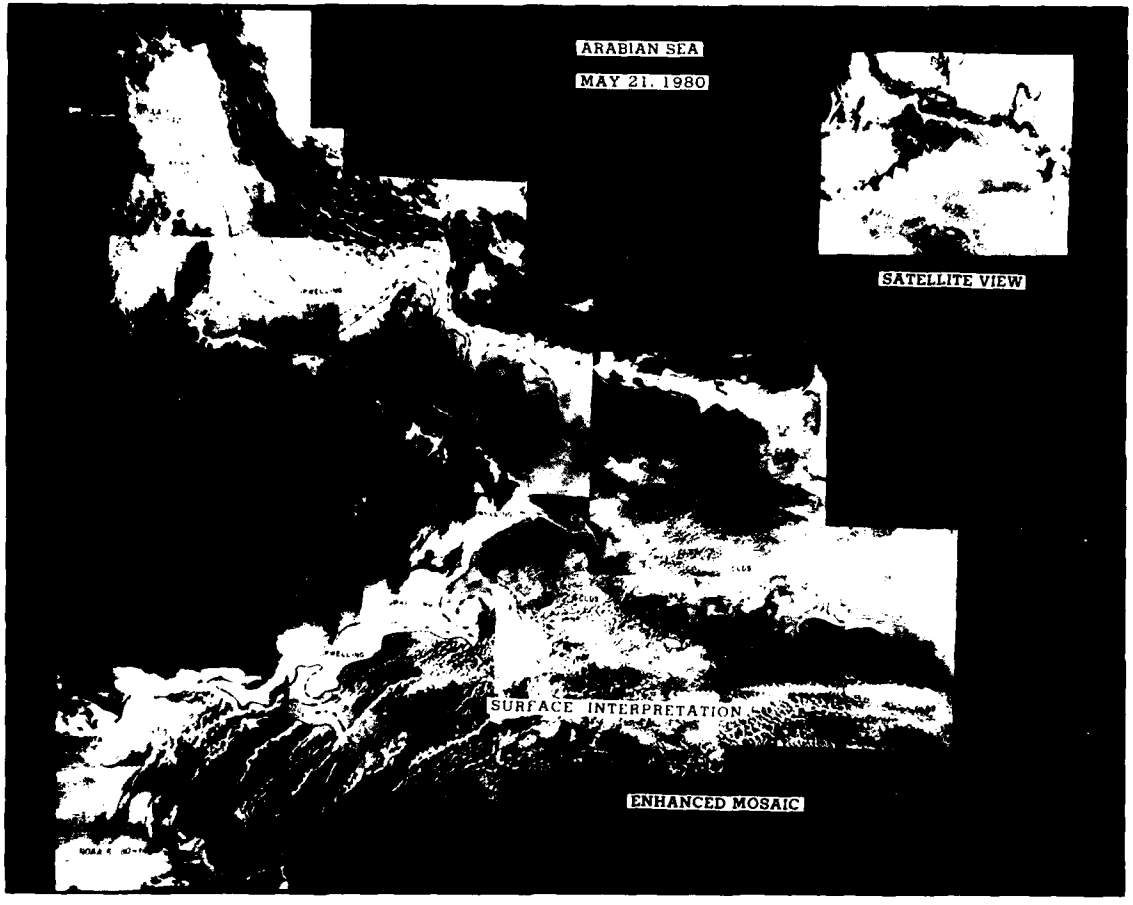

Figure 38. Arabian Sea Mosaic with Interpretation, 21 May 1980.

The composite of enhanced images shown in Figure 28 is shown here with a composite of surface interpretations for each image. Relative flow is indicated by arrows, and strong and weak fronts are indicated by solid and dashed lines respectively. Shear flow is indicated by a row of "x's". Upwelling regions are designated.

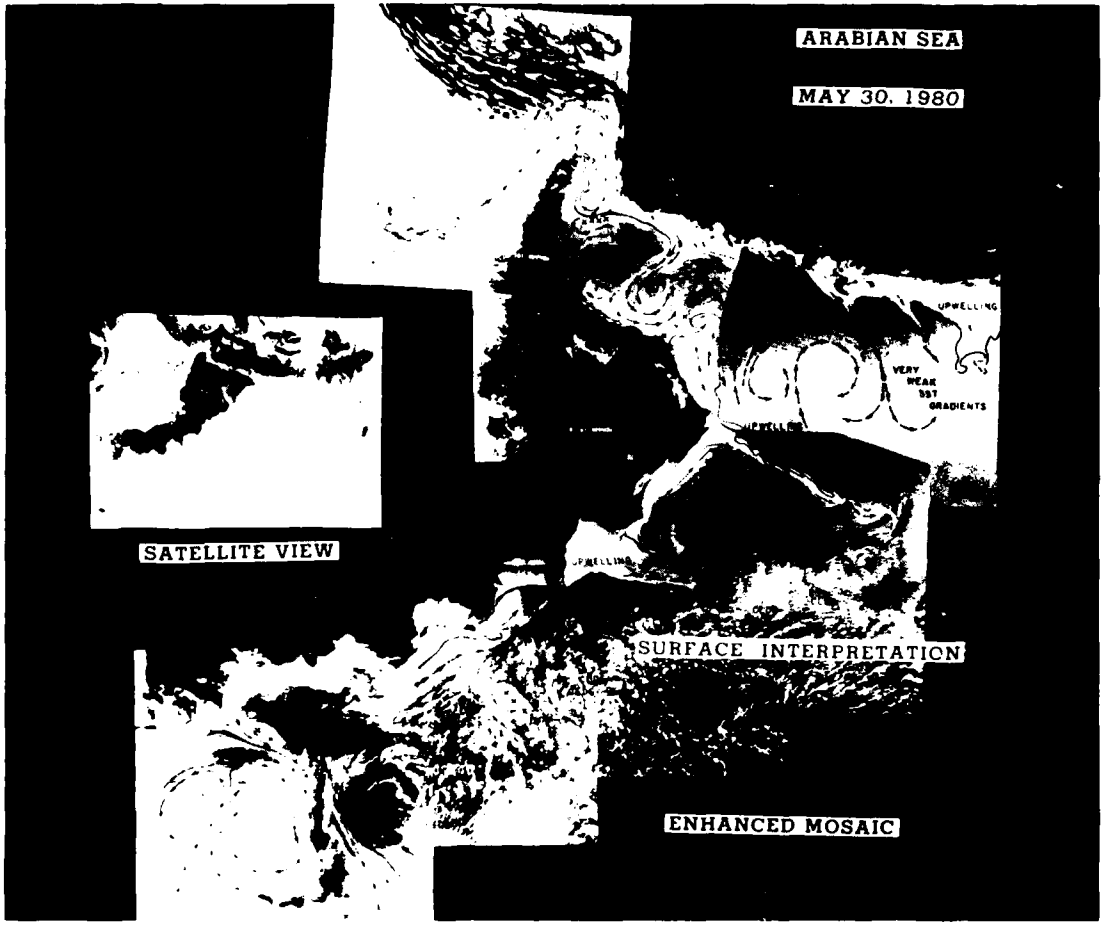

Figure 39. Arabian Sea Mosaic with Interpretation, 30 May 1980.

The composite of enhanced images shown in Figure 29 is shown here with a composite of surface interpretations for each image. Relative flow is indicated by arrows, and strong and weak fronts are indicated by solid and dashed lines respectively. Shear flow is indicated by a row of "x's". Upwelling is designated. (A poor alignment of lines indicating fronts occurred in the printing process.)

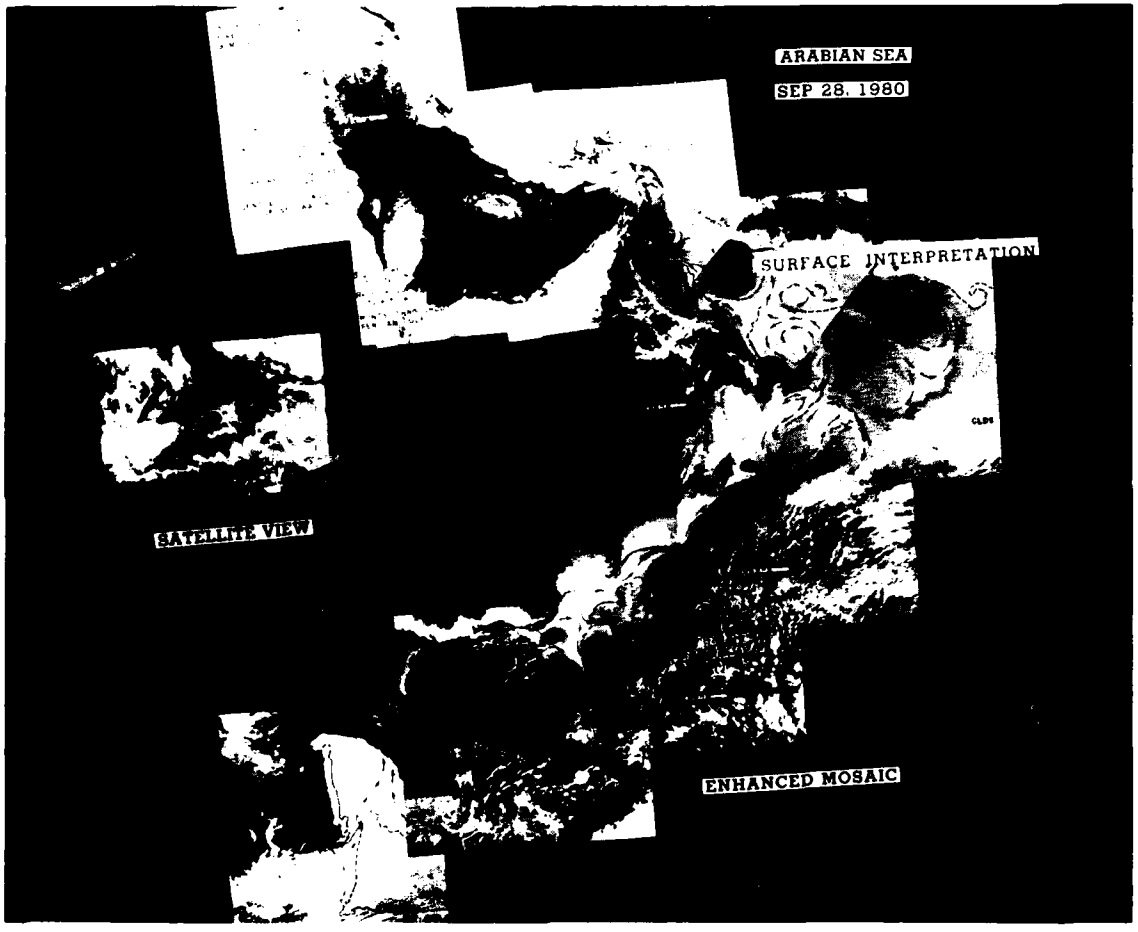

Figure 40. Arabian Sea Mosaic with Interpretation, 28 September 1980.

The composite of enhanced images shown in Figure 30 is shown here with a composite of surface interpretations for each image. Relative flow is indicated by arrows, and strong and weak fronts are indicated by solid and dashed lines respectively.

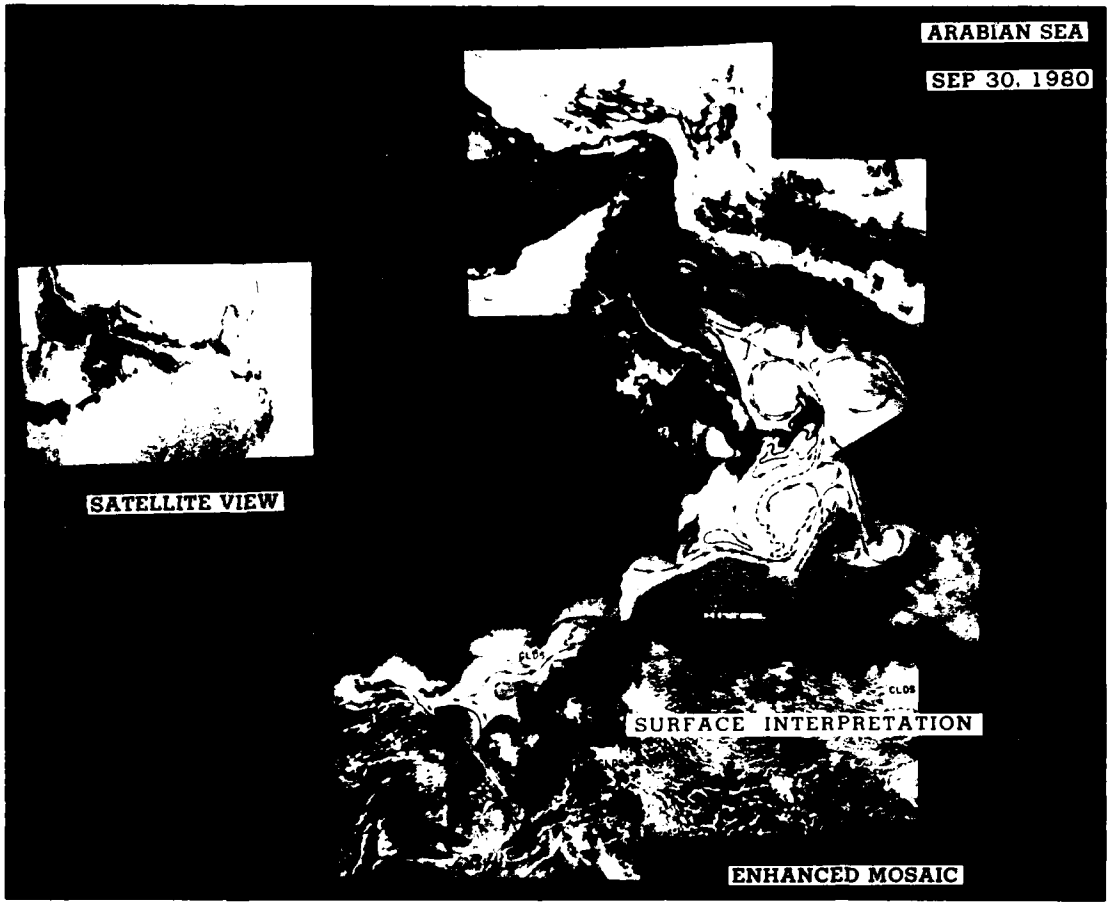

Figure 41. Arabian Sea Mosaic with Interpretation, 30 September 1980.

The composite of enhanced images shown in Figure 31 is shown here with a composite of surface interpretations for each image. Relative flow is indicated by arrows, and strong and weak fronts are indicated by solid and dashed lines respectively.

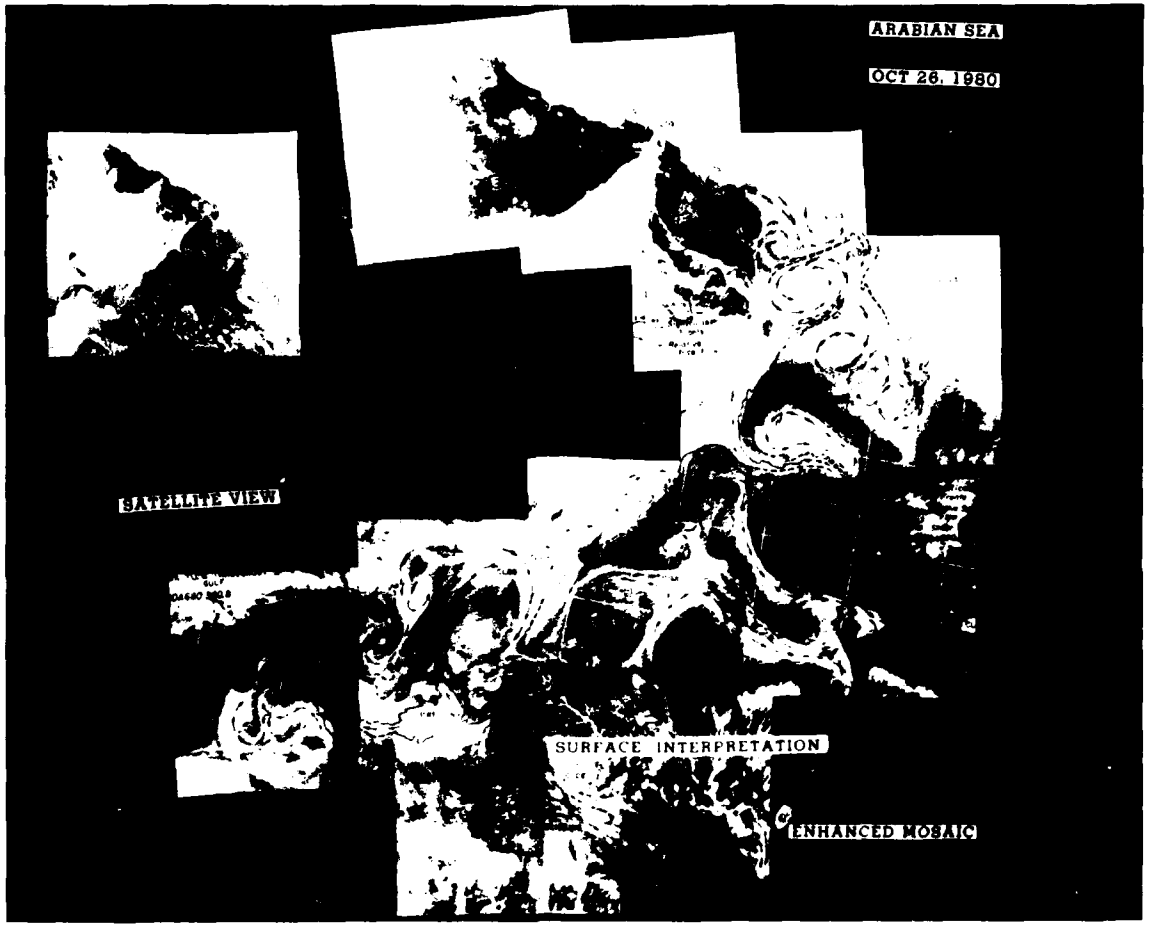

Figure 42. Arabian Sea Mosaic with Interpretation, 26 October 1980.

The composite of enhanced images shown in Figure 32 is shown here with a composite of surface interpretations for each image. Relative flow is indicated by arrows, and strong and weak fronts are indicated by solid and dashed lines respectively. The interpretations in this mosaic are described in more detail in Figures 15 through 25.

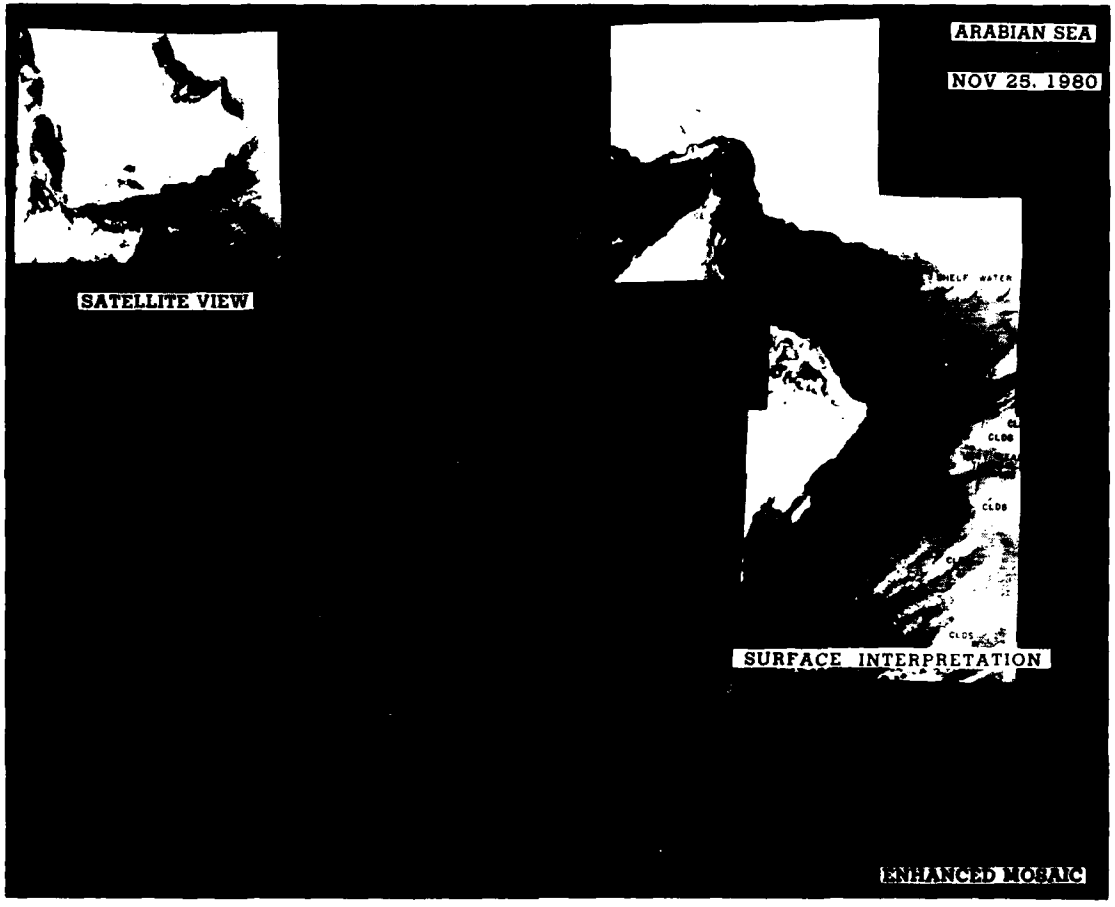

Figure 43. Arabian Sea Mosaic with Interpretation, 25 November 1980.

The composite of enhanced images shown in Figure 33 is shown here with a composite of surface interpretations for each image. Only weak surface features are indicated.

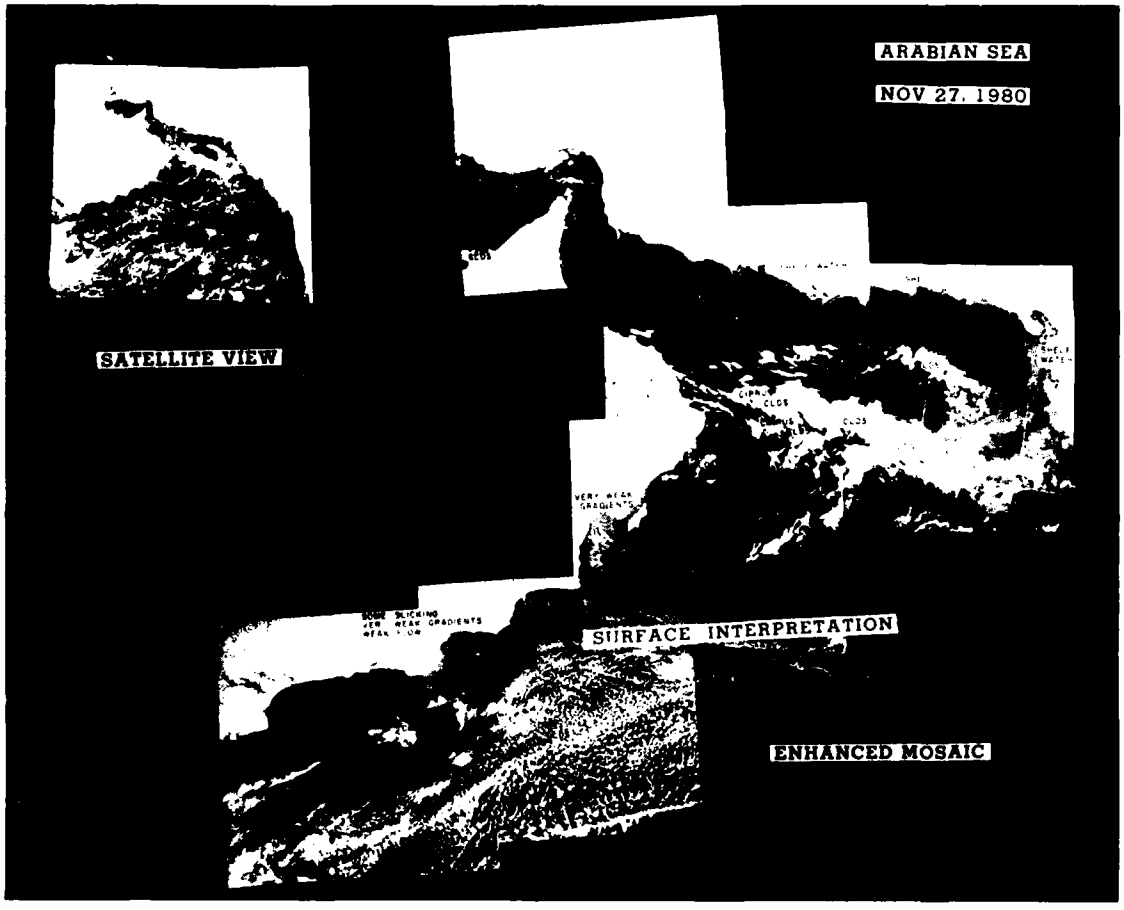

Figure 44. Arabian Sea Mosaic with Interpretation, 27 November 1980.

The composite of enhanced images shown in Figure 34 is shown here with a composite of surface interpretations for each image. Clouds dominate the field of view with some weak thermal features indicated on the ocean surface.

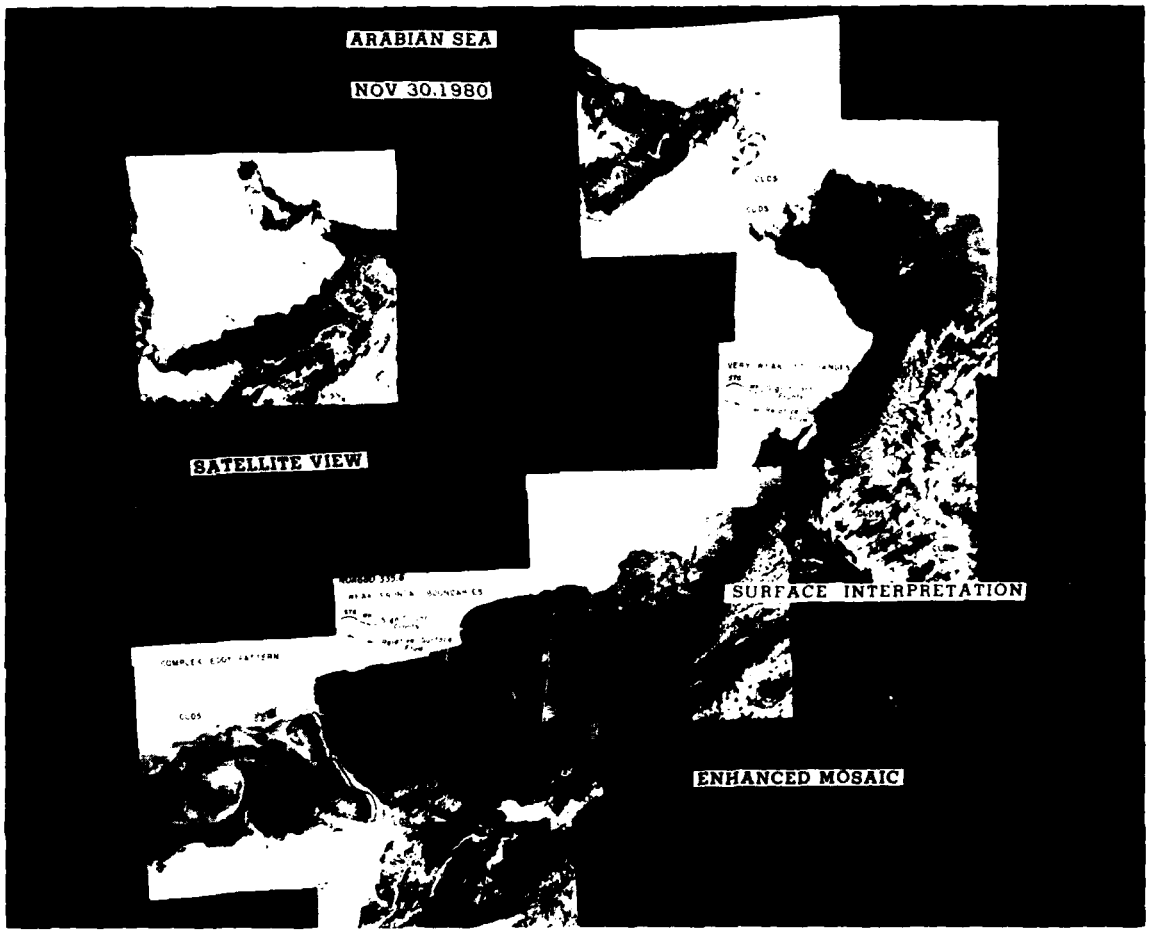

Figure 45. Arabian Sea Mosaic with Interpretation, 30 November 1980.

The composite of enhanced images shown in Figure 35 is shown here with a composite of surface interpretations for each image. Relative flow is indicated by arrows, and strong and weak fronts are indicated by solid and dashed lines respectively. (A poor alignment of lines indicating fronts occurred in the printing process.)


FILMED